Protoplasma (2021) 258:1231–1249
https://doi.org/10.1007/s00709-021-01644-y

ORIGINAL ARTICLE

The effects of osmotic stress on the cell wall-plasma membrane domains of the unicellular streptophyte, *Penium margaritaceum*

David S. Domozych[1] · Li Kozel[1] · Kattia Palacio-Lopez[2]

Received: 8 January 2021 / Accepted: 1 April 2021 / Published online: 30 April 2021

Abstract

Penium margaritaceum is a unicellular zygnematophyte (basal Streptophyteor Charophyte) that has been used as a model organism for the study of cell walls of Streptophytes and for elucidating organismal adaptations that were key in the evolution of land plants.. When *Penium* is incubated in sorbitol-enhance medium, i.e., hyperosmotic medium, 1000–1500 Hechtian strands form within minutes and connect the plasma membrane to the cell wall. As cells acclimate to this osmotic stress over time, further significant changes occur at the cell wall and plasma membrane domains. The homogalacturonan lattice of the outer cell wall layer is significantly reduced and is accompanied by the formation of a highly elongate, "filamentous" phenotype. Distinct peripheral thickenings appear between the CW and plasma membrane and contain membranous components and a branched granular matrix. Monoclonal antibody labeling of these thickenings indicates the presence of rhamnogalacturonan-I epitopes. Acclimatization also results in the proliferation of the cell's vacuolar networks and macroautophagy. *Penium*'s ability to acclimatize to osmotic stress offers insight into the transition of ancient zygnematophytes from an aquatic to terrestrial existence.

Keywords Osmotic stress, · Acclimatization, · Hechtian strands, · Pectin, · Wall

Introduction

Plant cell development is the expression of a highly coordinated series of subcellular events that occurs over specific periods of time and includes such phenomena as cell expansion, division, and morphogenesis (Landrein and Ingram 2019; Pierre-Jerome et al. 2018; Wang and Ruan 2013). During various stages of development, the activation/expression of specific gene sets define and coordinate the dynamics of subcellular and metabolic processes. These events are also highly sensitive to abiotic and biotic stress and modulate accordingly (Abdul Malik et al., 2020; Zhu 2016; Feng et al. 2016; Osakabe et al. 2013; Wang and Ruan 2013). Many of the specific signals produced by external stress agents are received, transduced and "communicated" to the cell interior by components of the plasma membrane (PM) and cell wall (CW) domains. The plant CW is a fiber reinforced hydrogel consisting of meshworks of cellulose microfibrils associated with an array of polysaccharides, proteins and phenolic polymers (Ali and Traas 2016; Liu et al. 2015; Wallace and Fry 1994). The CW provides a rigid protective boundary around the protoplast and also serves as a major sensory platform for reception and transduction of external signals (Sugimoto-Shirasu et al. 2018; Novakovic et al. 2018; Bashline et al. 2014). Communication between the external habitat, the CW and protoplast is also dependent upon a diverse array of proteins that reside in the PM (Rodriguez-Furlan et al., 2019; Novakovic et al. 2018; Liu et al. 2015; Luschnig and Vert, 2014; Komatsu et al. 2007). These proteins receive external signal input from the habitat and/or CW and transduce/direct them to specific internal loci such as the nucleus, endomembrane system or cytoskeletal network. Other PM proteins are critical for defining specific sites for secretion of CW matrix components (e.g., pectins, hemicelluloses) and for the biosynthesis of cellulose microfibrils, i.e., events central to plant cell expansion and morphogenesis (Polko and Kieber 2019; Kim and Brandizzi 2014; Maleki et al. 2016).

Handling Editor: Andreas Holzinger

✉ David S. Domozych
ddomoz@skidmore.edu

[1] Department of Biology and Skidmore Microscopy Imaging Center, Skidmore College, Saratoga Springs, NY 12866, USA

[2] Department of Evolution, Ecology and Organismal Biology, The Ohio State University, Columbus, OH, USA

Liquid water and more specifically, its movement across biological membranes, are fundamental to virtually all of the dynamics of a cell. In most walled plants and algae, water inside the cell exerts outward pressure (turgor pressure) on the cell periphery thus providing a physical force for expansion (Hill et al. 2012). This force is counteracted and controlled by the rigid CW (wall pressure). During development, the "loosening" of particular CW zones via enzymatic activity and/or secretion/insertion of new wall polymers allows for controlled expansion at these zones (Haas et al. 2020; Zhang and Zhang 2020; Cosgrove 2018; Zwieka et al. 2015; Pietruszka, 2013; Zonia and Munnik 2011, 2007). CW expansion and corresponding cell expansion may occur around the whole cell, i.e., diffuse cell expansion (Cosgrove 2016) or may be localized at one or a few zones that then manifest in polar growth expansion (Dehors et al. 2019; Bidhendi and Geitmann 2018; Domozych et al. 2013). If a plant cell is incubated in a hyperosmotic solution, the high water potential in the cell directs the movement of water out of the cell where a low water potential exists (Cheng et al. 2017). This causes a decrease in protoplast volume or plasmolysis and represents one of the major responses of a plant cell to osmotic stress. Plasmolysis is often observed in plant cells experiencing high salt exposure, low water conditions and cold stress (Yoneda et al. 2020; Cheng et al. 2017; Lang et al. 2014), i.e., conditions common to many terrestrial and freshwater aquatic habitats (e.g., wetlands). Plasmolysis is accompanied by significant subcellular changes and after long periods, may result in cell death. However, after this initial response to osmotic stress, many plant cells alter their metabolism and subcellular architecture/dynamics and resume expansion/growth, i.e., acclimatization (Novakovic et al. 2018). This is a critical survival strategy for plants living in terrestrial habitats.

Approximately 500+ mya, an ancestor of modern day Zygnematophycean algae, (Zygnematophyceae, Streptophyta or Charophyta) successfully colonized land and from this ancient stock evolved land plants (Buschmann and Holzinger, 2020; Becker et al. 2020; Wang et al., 2020a; Delwiche and Cooper 2015). Though little fossil data is available, it is believed that the habitats where this most likely occurred were shallow wetlands that experienced frequent periods of drying, i.e., also habitats of many modern day zygnematophytes (i.e., taxa belonging to the Zygnematophyceae). Zygnematophytes have adapted multiple mechanisms to cope with this osmotic stress (Furst-Jansen et al. 2020) including changes to chloroplast/photosynthetic dynamics, production of osmolytes, the transformation into specialized resting cells and, modulating CW structure and biochemistry (Steiner et al. 2020; Herburger et al. 2019, 2018, 2015; de Vries et al. 2018; De Vries and Archiblad, 2018; Herburger and Holzinger 2015; Holzinger and Pichrtova, 2016; Rippin et al. 2017; Lütz-Meindl 2016; Holzinger and Karsten 2013). The CWs of extant zygnematophytes have been shown to have polymers with notable similarity in composition and accompanying biosynthetic machinery to that found in land plants (Jiao et al. 2020; Sørensen et al. 2011, 2010). These features make extant zygnematophytes highly desirable organisms for investigating the effects of stress and subsequent response mechanisms not only in light of evolution but also for providing insight into cell and CW adaptations to osmotic stress in plants.

Recently, the unicellular zygnematophyte, *Penium margaritaceum*, has become a valuable organism for studying the cell biology of zygnematophytes especially CW-related phenomena. *Penium* produces only a primary CW that contains many polymers similar to those found in land plants (Domozych et al. 2014, 2007). Its outer CW layer consists of a distinct calcium (Ca^{2+})-complexed homogalacturonan (HG) lattice that is highly malleable when synthesized during stress conditions (Palacio-Lopez et al., 2020). The components of the CW and the exopolymeric mucilage or EPS (i.e., extracellular polymeric sunstance) secreted by *Penium* are synthesized and processed by a highly elaborate endomembrane system (Domozych et al. 2020; Ruiz-May et al. 2018) and secreted at specific loci of the cell periphery. Analysis of these features and events is directly accessible for analysis using various microscopy-based protocols. Furthermore, *Penium*'s genome has been recently sequenced (Jiao et al. 2020) and the putative molecular adaptations for response to stress have been initially identified. In this study, we examined the affects of experimentally-induced osmotic stress on the cell with special emphasis on the CW and PM domains. We examined both short term and long term treatments, i.e., acclimatization. Osmotic stress causes significant changes including the production of Hechtian strands, the alteration of the HG lattice of the CW and the formation of distinct peripheral thickenings found between the CW and PM.

Materials and methods

Penium culture maintenance

Penium margaritaceum Brébisson (Skidmore College Algal Culture Collection, clone Skd#8) was maintained in sterile liquid cultures of Woods Hole Medium (Rydahl et al. 2015; Domozych et al. 2007) supplemented with soil extract (WHS), pH 7.2 at 18°C +/−1.5°C in a photoperiod of 16-h light/8-h dark with 74 μmol photons m^{-2} s^{-1} white fluorescent light. The cells were subcultured every week, and cells from log-phase cultures (7- to 14-day-old cultures) were used for the experiments.

Experimental protocols

Cells were collected from liquid cultures, gently pelleted by centrifugation at 500×*g* (1 min) and washed three times in WHS before experimental treatments. For long-term sorbitol treatment or acclimatization experiments, cells were incubated in 200 mM sorbitol (Sigma-Aldrich; St. Louis, MO, USA ; 211 mOsm) in WHS for 1-10 days and cultured as above. Osmolarity was measured with a Vapro Vapor Pressure Osmometer

Model 5600. Aliquots of culture were removed at 24, 48, 72, 96 h and 7 d and processed or light and electron microscopy. For induction of Hechtian strands, cells were treated with 300 mM sorbitol (315 mOsm)in WHS for 1 min, 5 min, 30 min and 4 h. Cells were collected and processed for spray freezing/freeze substitution (see below). For Polyethylene Glycol (PEG) treatment, cells were treated with 15% PEG (mw. 3,500; Sigma-Aldrich; St. Louis, MO, USA) for 72 h and 6 d before removal for analysis. For assessment of CW and cell expansion under experimental conditions, aliquots of treated cells and control cells were harvested at 24, 48, and 72 h, labeled with JIM5-TRITC using the double immunofluorescence protocol as described in Domozych et al. (2007). New CW growth was monitored using fluorescence light microscopy (FLM) and the protocol described in Domozych et al. (2009). 50 cells from triplicate samples were examined for each treatment at 24, 48, and 72 h. For recovery experiments, treated cells were collected, washed three times with WHS, placed back in fresh WHS and cultured as described above.

Labeling protocols for vacuoles, nucleus, cytoskeleton, and CW

All chemicals were obtained from either Sigma-Aldrich (St. Louis, MO, USA; Neutral Red) or Molecular Probes (Eugene, OR, USA; SYTO9, Calcofluor) or BioSupplies (Australia; aniline blue). Cell labeling was performed in the dark at room temperature and with constant gentle shaking. Cells were collected and washed three times with WHS to remove residual EPS from the cell surface that might interfere with labeling. Washed celles were then incubated in fresh WHS medium containing 10 μg/ml solution of Neutral Red for 30 min (for vacuole labeling) in the dark, or 30 min in the dark with 1mg/mLof SYTO9 (for nucleus labeling) or 30 min in the dark with 10 μg/mL Caclofluor (for cellulose and ß-glucans) or 30 min in the dark with 1 μg/mL of aniline blue (for ß1-3 glucans). The cells were subsequently washed three times with WHS. Cells were then viewed with differential interference contrast (DIC) microscopy, FLM or confocal laser scanning microscopy (CLSM). Screening for the presence of microfilaments and microtubules entailed the labeling techniques employed in Ochs et al. (2014). For CW labeling, cells were harvested washed labeled with JIM5-TRITC using the double immunofluorescence protocol described in Domozych et al. (2014).

DIC (differential interference contrast), FLM (fluorescence light), and CLSM (confocal laser scanning microscopy) imaging

For routine-, DIC-LM and FLM, cells were viewed with an Olympus BX60 or BX63 microscope (Olympus America Inc., Melville, NY, USA) equipped with an Olympus DP73 digital microscope camera, using DP Controller 3.2.1.276 software. DIC images were obtained using U Plan Apo 40 or 100× lenses. Confocal laser scanning microscopy (CLSM) was performed with an Olympus FluoView™ 1200 Confocal Microscope using Fluoview 5.0 with O3D software. FLM and CLSM images were obtained with a U Plan Apo 60 lens with fluorescein isothiocyanate (FITC) or tetramethylrhodamine isothiocyanate (TRITC) filter sets.

Field emission scanning electron microscopy (FESEM)

Cells were collected, washed three times with WHS and shaken in 0.05% Triton-X in WHS at 4°C for 10 min. The cells were then freeze shattered (Palacio-Lopez et al. 2020; Wasteneys et al., 1997), washed extensively with deionized water, frozen in liquid nitrogen and freeze dried. The dried cells were then brushed onto double-sided sticky tape on a Cambridge stub (EMS, Ft. Washington, PA) and sputter coated with gold-palladium (25 s). FESEM imaging was performed using a ThermoFisher Quattra FESEM. High-resolution imaging employed a secondary electron detector with a 5-kV accelerating voltage, 2.5 spot size, and a 10-mm working distance under high vacuum conditions

TEM

Cells were prepared for TEM using freeze spraying techniques described in (Rydahl et al. (2015; Domozych et al. 2007). Immunogold labeling of thin sections employed mAbs from Plant Probes, Leeds, UK (JIM5, JIM13, LM11, LM15). http://www.plantprobes.net), the Complex Carbohydrate Research Center (CCRC-M80) of the University of Georgia, USA, BioSupplies, Australia (400-2) and from Dr Marie-Christine Ralet (INRA-RU1) of INRAE, Nantes, France. The protocol described in Domozych et al. (2007) was used for labeling. Immunogold labeled and regular sections were imaged on an Hitach HT7800 TEM at 120 kV

Results

General cytological features

Penium's typical (i.e., control) phenotype is an elongate cylinder with two rounded poles (Fig. 1a). Cells measure 150–225 μm in length and 17 μm in width at the cell center or isthmus. Throughout most of the cell cycle, the isthmus contains the nucleus and is the site of CW expansion (Fig. 1b; see also Davis et al. 2020; Domozych et al. 2014, 2009). JIM5, a monoclonal antibody (mAB) with specificity toward de-esterified HG, labeled the outer layer of the CW (Fig. 1c, d, e; Suppl Table 1). *Penium* secretes and incorporates new CW components into a narrow zone at the isthmus that in turn, push older CW toward the two poles (Fig. 1c). JIM5 labeling also highlighted the distinct HG lattice projections of the outer CW layer that cover almost the entire cell surface (Fig. 1e). FESEM (Fig. 1f) and TEM (Fig. 1g) imaging shows that the outer HG lattice consists of a network of branched fibers that cover the CW surface and occasionally rise up off the surface, fuse and produce distinct projections.

Phenotype changes upon acclimatization to long-term sorbitol incubation

A major goal of this study was to investigate the ways that the CW/PM domains and cell adapted to long term exposure (acclimatization) to osmotic stress . We initiated this work by screening cell and CW alterations in cells growing in varying concentrations of sorbitol (150–350 mM). For acclimatization studies, we chose 200 mM sorbitol as it causes distinct but reversible changes to cells in cultures 24 h to 7 d old. There were 48–72-h-old cultures ultimately selected for further investigations. Significant changes in cell shape and CW architecture occured in cells incubated in 200 mM sorbitol for 48 h or longer. At 72 h of incubation, cell shape transformed (Fig. 2a) to a highly elongate if not "filamentous" phenotype. Chloroplast positioning and general ultrastructure were not notably changed during the treatments. The most notable alteration was at the isthmus zone (Fig. 2b), the site of CW expansion. The CW became highly irregular and the isthmus was filled with dense cytoplasm. In cells that divided right before incubation in 200 mM sorbitol, the expanding poles of the daughter cells

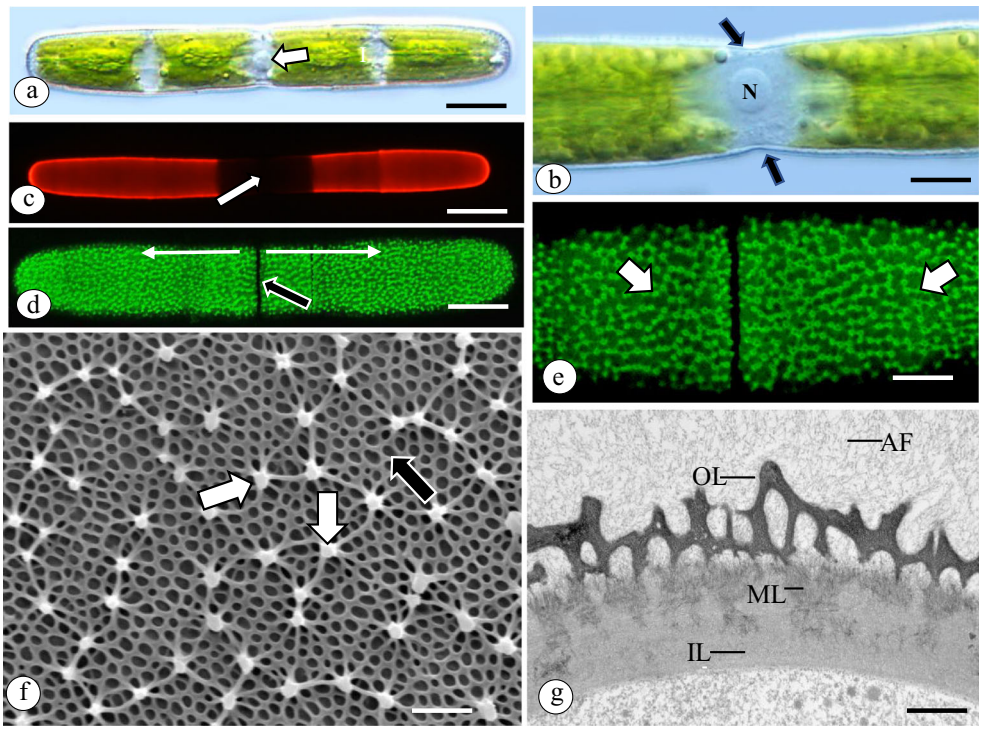

Fig. 1 Cell and CW features. **a** *Penium* is an elongate cylindrical unicell with rounded poles. A central isthmus zone (arrow) is flanked by the two semi-cells containing the chloroplasts. **b** The isthmus contains the nucleus (N) and is the site of CW deposition (arrows) and CW/cell expansion. **c** When cells are labeled with JIM5-TRITC and placed back into culture, newly deposited cell wall growth is observed as dark zones (arrow) in the isthmus between the labeled wall at the polar zones (see also Domozych et al. 2014). **d** JIM5-TRITC labeling of the HG lattice of projections on the CW surface (black arrow). HG is secreted at the isthmus and pushes older CW outward toward the two poles (white arrows). **e** Magnified view of the JIM5-labeling HG projections of the outer layer of the CW. **f** FESEM image of the HG projections (arrows) that make up the outer wall layer lattice. Projections arise from a basal layer of CW surface fibers (black arrow). **g** TEM imaging of the CW. The outer layer (OL) consists of the HG lattice. This layer is embedded into a medial layer (ML) that resides in an inner layer (IL) of cellulose. The adhesive fibrils (AF) of the cell surface arise from the outer layer. **a** DIC image, 15.5 μm, **b** DIC image, 8 μm, **c** FLM image, 25 μm, **d** CLSM image, 12.5 μm, **e** CLSM image, 6 μm, **f** FESEM image, 1.1 μm, **g** TEM image, 480 nm

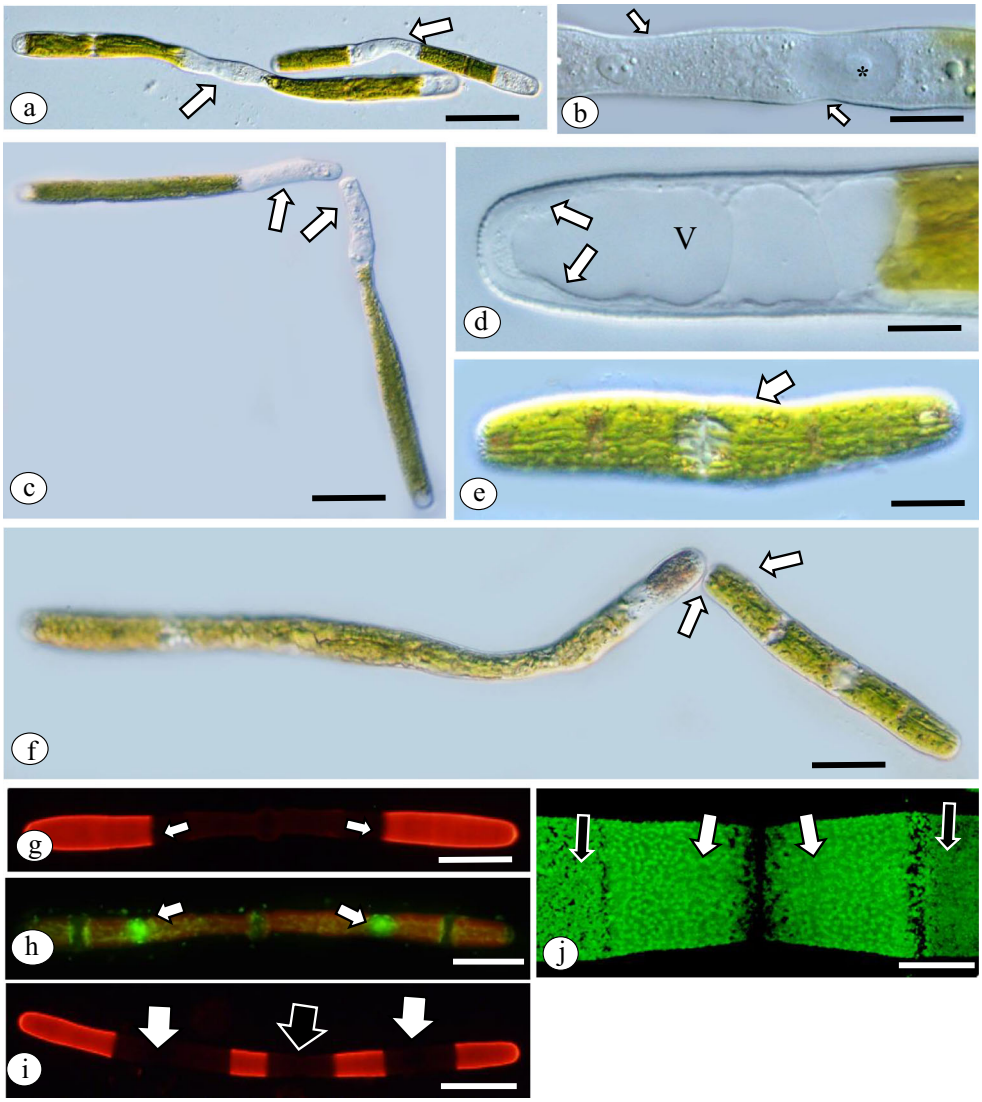

Fig. 2 Cell alterations during sorbitol acclimatization. **a** After 72 h in 200 mM sorbitol, cells expand but do not divide and yield elongate cells that are "filamentous". Most notable changes are at the isthmus (arrows). **b** The altered isthmus contains the nucleus. (*) and has a irregular CW (arrows). **c** In cells that recently divided just before incubation in sorbitiol, the expanding poles of daughter cells take on irregular shape (arrows). **d** Acclimatization for 96 h also causes the cell to fill with vacuoles (V) most notably at the polar zones. A thick peripheral layer of cytoplasm is also noted at the poles (arrows). **e** When cells are washed free of sorbitol, cell begin to divide within 12 h. The daughter cells are approximately 25% shorter than control cells (arrow). **f** Post-recovery daughter cells emerge via cell division at the peripheries of the elongate filament-like cells (arrows). **g** JIM5 labeled cell treated incubated for 24 h in 200 mM sorbitol. Note that cell wall expansion continues durting treatment (arrows). **h** During acclimatization, mitosis occurs, cytokinesis does not and the daughter nuclei migrate to opposite ends of the filament (arrows). **i** CW expansion occurs where the daughter nuclei have migrated (arrows). **j** Recovery of cell 24 h after acclimatization in sorbitol. The new HG lattice (white arrows) forms at the isthmus while the CW formed prior to recovery (black arrows) has an altered lattice. **a-f=** DIC images, **g-i**=FLM images, j= CLSM image. **a** 50 μm, **b** 10.7 μm, **c** 50 μm, **d** 8.1 μm, **e** 15 μm, **f** 30 μm, **g** 34 μm, **h** 50 μm, **i** 50 μm, **j** 12.5 μm

were the sites where cell shape and CW alterations occured (Fig. 2c). After acclimatization for 96 h or longer, the cells also became highly vacuolate, most notably at the polar regions (Fig. 2d). Cells recovered from treatment upon removal of sorbitol by extensive washing with fresh growth medium and placement back in culture. We noted that virtually all cells divide within 12 h but the daughter cells were approximately 25% +/− 5% smaller than control daughter cells. This was based on three different counts of 50 recovery cells vs 50 cells from control (untreated) cultures. The daughter cells displayed curving at one semi-cell (Fig. 2e) and the normal cylindrical shape at the other. We interpret the former to be the zone where post-recovery expansion occured and the latter being where the shape and CW alterations occurred during acclimatization. Cell division after recovery also occured at the periphery of the filament-like phenotype and not in the altered cell center (i.e., at the terminal nucleus of the multinucleate

phenotype; Fig. 2f). Subsequent cell divisons during recovery yielded the typical cylindrical daughter cells. JIM5 and SYTO9 labeling were used to monitor changes to CW expansion and positioning of the nucleus. In pre-cytokinetic desmids, post-mitotic nuclei move to the future isthmus zones of daughter cells (Domozych et al. 2009). Cytokinesis then takes place at the isthmus zone of the parent cell. In this study, cell and CW expansion were not inhibited by sorbitol incubation (Fig. 2g) and in fact, new CW expansion rates were 30% +/−5% higher than that of control cells after 24 and 48 h treatment. Also during acclimatization, mitosis, and nuclei migration occured (Fig. 2h) but cytokinesis did not (Fig. 2i). This resulted in the highly elongate, "filamentous" phenotype. Upon recovery treatment, and HG lattice with the typical projections formed at the isthmus (Fig. 2j). Finally, if post-recovery cells were placed back in hypersosmotic medium, the changes to the cell and CW as noted above reoccued.

Sorbitol-induced formation of Hechtian strands

In order to elucidate Hechtian strand formation during sorbitol treatment, we incubated cells in 300 mM sorbitol for 1, 3, 10, 60, and 240 min. This was the minimum sorbitol concentration that caused the strands to form. After 1 min of treatment, shallow invaginations of the PM appeared around the cell periphery and contained mostly small membranous units, i.e., Hechtian strands (Fig. 3a; Suppl. Fig 2). The strands measured 47 +/− 5 nm in diameter with varying lengths of up to 5 μm (Fig. 3b, c). Actin cables, microtubules or endoplasmic reticulum (ER) were not observed in these strands. The strands emerged from the PM and attached to the inner layer of the CW (Fig. 3d). The highest number of Hechtian strands were observed in cells treated for 5 min (Fig. 3e, f). We analyzed serial TEM micrographs of 200 nm-sections of 25 cells incubated for 5 min and estimated that 1000–1500 strands are found per cell. It is important to note though that our counts were not meant to provide exact numbers of strands as they are fragile and their numbers do vary over time. Our goal was simply to provide snapshot of the distinctly large number of Hechtian strands that form in response to this osmotic stress. We also measured Hechtian strand frequency on the PM in 100 nm sections of 25 cells. Strands emerged from the PM every nm 300 +/- 25 nm (Fig. 3g) and a notable periodicity emerging just off the PM was apparent (Fig. 3h). After 60 min of incubation, the strands took on a beaded appearance that most likely represented strand breakdown (Fig. 3i). Strands were not present after treatments of 120 min or longer. During treatment of 60 min, invaginations or pockets of circular membrane components and other inclusions appeared at the cell periphery (Fig. 3j; see below). Hechtian strand membrane-breakdown products were likely the source of some of these components. In recovery experiments of cell incubated for less than 60 min in sorbitol, protoplasts expanded quickly and the determination of the fate of the strands was not possible.

Sorbitol-induced changes to CW architecture

Sorbitol-induced cell shape alterations were accompanied by notabable changes to the CW after 24 h or longer incubation.. In those areas surrounding the CW expansion zone, i.e., the isthmus, the typical outer CW layer containing the HG lattice was not apparent (Fig. 4a) and also was thinner than the CW formed prior to incubation (Fig. 4b). A second distinct feature of acclimatization to sorbitol incubation was the appearance of peripheral thickenings located just inside the CW (Fig. 4c). JIM5-labeling revealed significant changes to the HG lattice during acclimatization (4 days) including a significant reduction in labeling and the absence of the outer projections of the lattice (Fig. 4d, e). TEM examination of the altered CW showed that while the inner and medial CW layers appeared intact, the outer layer containing the lattice was much reduced and highly irregular (Fig. 4f). FESEM further revealed that the altered CW zones contained irregular patches of fibers that constituted the lattice base interspersed with fiber-free zones. No projections were noted during acclimatization (Fig. 4g, h).

The formation of peripheral thickenings during sorbitol acclimatization

When incubated in 200 mM sorbitol for 24 h, distinct thickenings appeared between the CW and PM (Fig. 5a). These thickenings exhibited a developmental pattern. After 5 min or longer of sorbitol incubation, the inclusions were filled with small membranous components (Fig. 5b) that most likely were Hechtain strands. After 24 h incubation, the thickenings contained "matrix" components of a fine granular consistency that was moderately osmiophillic (i.e., stained with osmium tetroxide; Fig. 5c). These matrix inclusions increased in size/number and became branched (Fig. 5d) after 72 h acclimatization. The thickenings also expanded inward into the cell and in some cells after 72 h, were invaded by channels of cytoplasm (Fig. 5e). In some inclusions formed after 72 h acclimatization, tufts of fibrillar material that connect with the inner CW layer became apparent (Fig. 5f). The fibrils were 4.5 nm in diameter and did not stain with either Calcofluor or aniline blue, indicating athe absence of B-glucans. In cells acclimatized for 96 h or longer, the thickenings contained multiple membrane inclusions interspersed with branched matrix material (Suppl. Fig. 3 a, b, c).

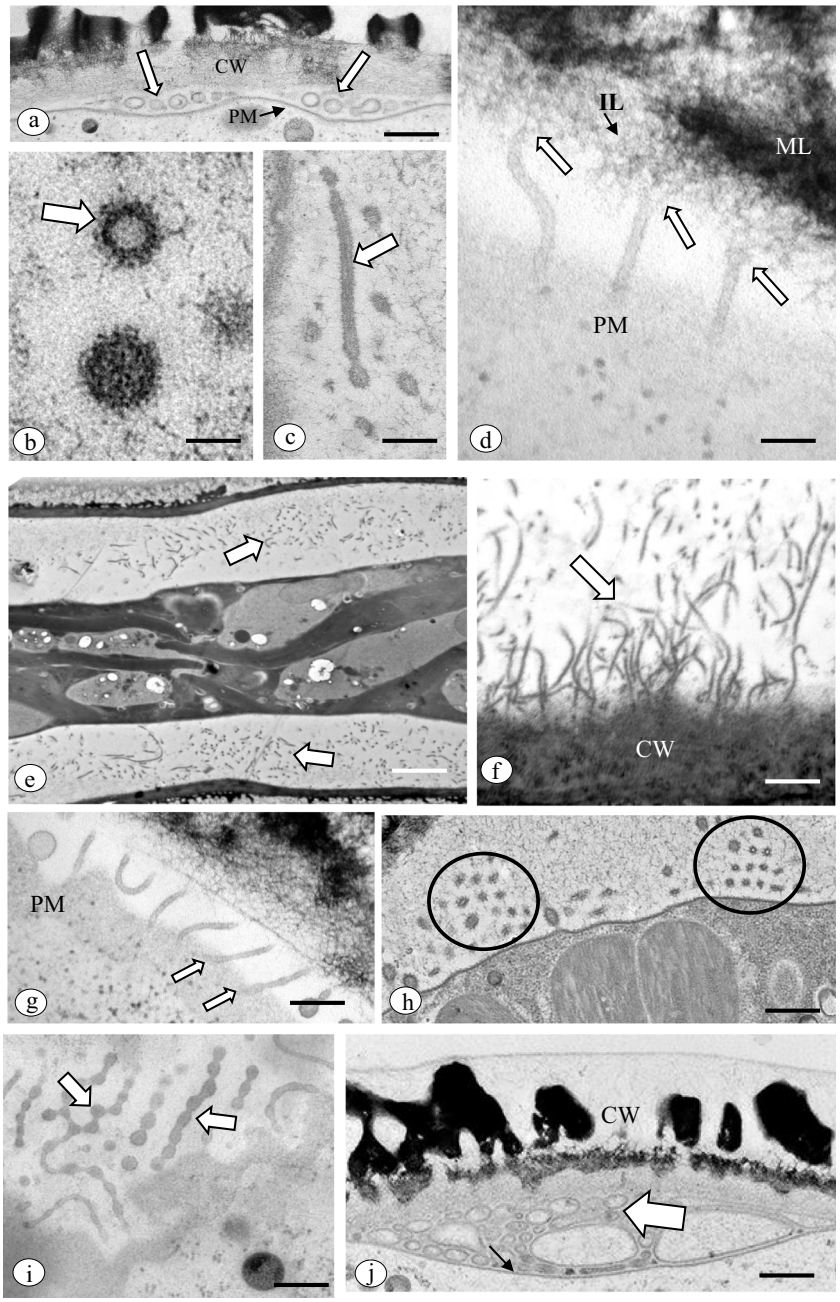

Fig. 3 Hechtian strand formation. **a** After 1 min of incubation in 300 mM sorbitol, Hechtian strands (arrows) appear in small invaginations of the plasma membrane (PM) just interior to the cell wall (CW). **b** Each strand (arrow) is 47 nm +/− 5 nm in diameter. **c** Strands (arrow) attain lengths of up to 5 μm and do not contain ER or cytoskeletal components. **d** Strands (arrows) arise from the plasma membrane PM and contact the inner fibrils of the inner layer (IL) of the cell wall (CW). The medial layer (ML) is also present. **e** The strands are stable during shorter incubation times (e.g., 5–20 min). 1500–2000 of strands (arrows) re estimated in each cell. **f** A high density of strands (arrow) make contact with the inner later of the cell wall (CW) after 5 min incubation. **g** After 5 min incubation strands (arrows) arise from the plasma membrane (PM). We estimate that strands are separated by 300 +/− 50 nm. **h** A regular periodicity of the strands may be observed just off the plasma membrane (PM) after 5 min incubation. **i** After longer incubation periods (60–240 min), the strands (arrows) transform and have a "beaded" appearance (arrows). **j** Strands (arrow) or remnants thereof are found in the peripheral invaginations (see also Fig. 5) situated between the cell wall (CW) and the plasma membrane (PM) (black arrow). All images= TEM, **a** 1.2 μm, **b 45** nm, **c** 200 nm, **d** 265 nm, **e** 2.75 μm, **f** 1 μm, **g** 600 nm, **h** 630 nm, **i** 250 nm, **j** 590 nm

In order to determine the constituents of the thickenings, we employed immunogold labeling using mAbs that recognize particular CW polymer epitopes. We chose antibodies that have been successfully used in labeling CW components in previous studies (Davis et al., 2020; Domozych et al. 2014: JIM5➔ de-esterified HG, JIM7➔ methyl esterified HG, LM6 ➔ arabinan, LM15➔ xyloglucan, LM11➔ arabinoxylan, INRA-RU1➔ rhamnogalacturonan-I or RG-I, CCRC-M80 ➔ RG-I and BS400-2➔ ß1-3 glucan). Supplementary Table 1 provdes a summary of the labeling. To highlight examples of positive and negative labeling, JIM5 (Fig. 6a) and BS400-2 (Fig. 6e) did not label the thickenings (see also Davis et al. 2020, Domozych et al. 2014 for CW labeling patterns). However, INRA-RU1 weakly labeled while CCRC-M80 strongly labeled the thickenings (Fig. 6c). In control cells, CCRC-M80 labeling was found at the interface of the PM and CW (Fig. 6d) while INRA-RUI labeled the medial layer of the CW (Fig. 6b; Domozych et al. 2014). Control labeling whereby the primary mAb was eliminated showed no labeling (Fig. 6f).

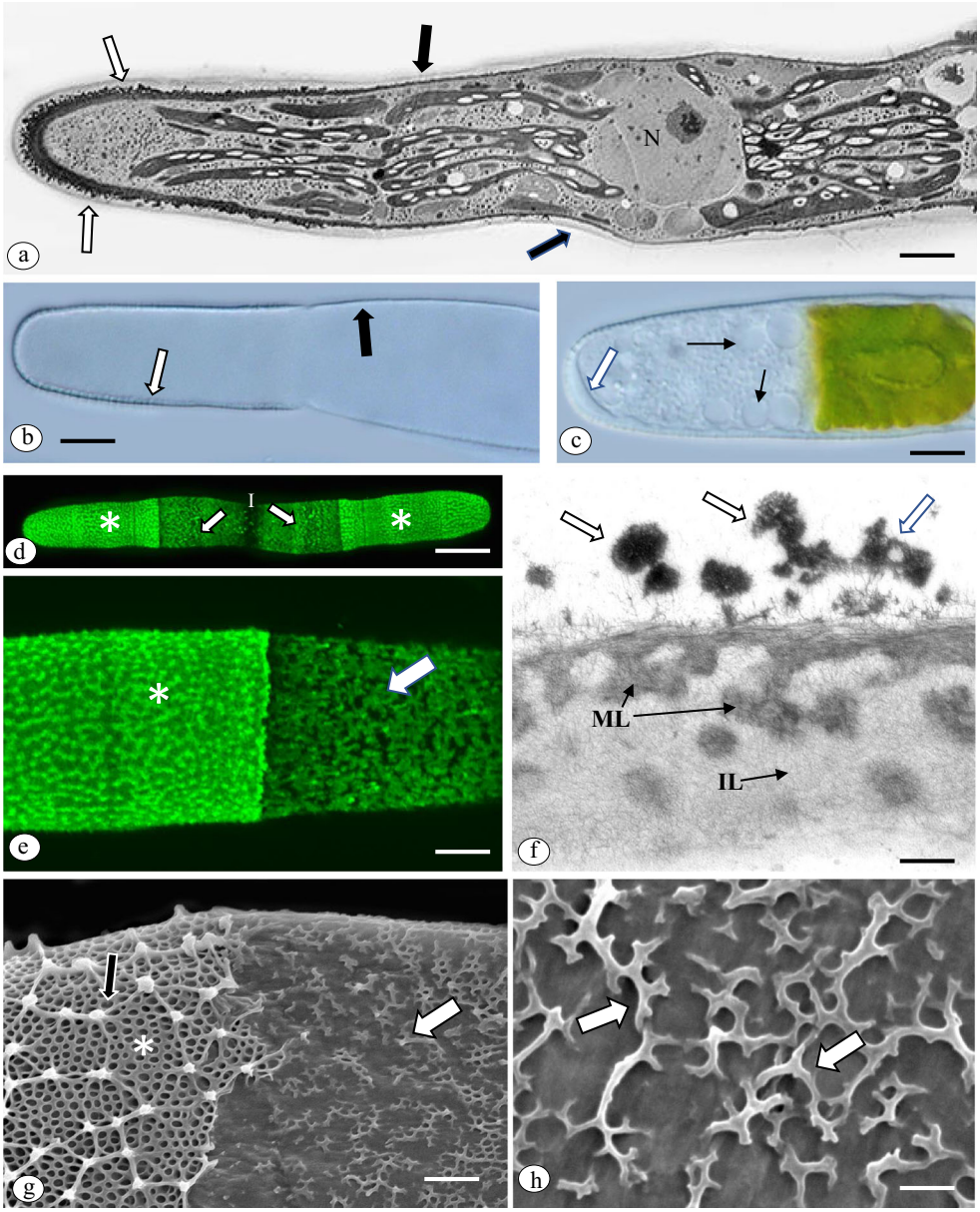

Fig. 4 Sorbitol-induced changes to the CW. **a** Incubation in 200 mM sorbitol for 72 reveals significant shape changes of the cell, most notably and the isthmus. Here, the altered CW (black arrows) lacks a discernable outer wall lattice and appears thinner than the CW formed before sorbitol incubation (white arrows). **b** The cell wall of a ruptured cell after 72-h incubation shows a distinct difference in thickness and structure the pre-existing wall (white arrow) with the altered cell wall (black arrows) formed during sorbitol incubation. **c** After 48-h incubation, the polar cytoplasm fills with vacuoles (black arrows) and also distinct thickenings or pockets (white arrow) located just interior to the CW. **d** and **e** JIM5-TRITC labeling of the CW of a cell incubated for 48 h shows the transformation of the lattice into an irregular coating at the isthmus zone (**d**, arrows; **e**, arrow). The typical lattice formed before incubation is also observed (*). **f** TEM image of the altered CW. While inner (IL) and medial (ML) layers are still present, the outer wall lattice (arrow) is much reduced and irregular (white arrows). **g** FESEM image of the transition from pre-exisiting wall (black arrow) to the altered CW (white arrow) formed during incubation for 48 h. The lattice is notably reduced and consists of patches of fiberes interspersed with open areas on the CW surface. **h** Magnified FESEM image of the altered CW region. Note the irregular network of fiber patches (arrows) and open zones on the CW surface. No projections are formed. **a** TEM image, 9.7 μm, **b** DIC image, 9.3 μm, **c** DIC image, 7.3 μm, **d** CLSM image, 17 μm, **e** CLSM image, 5.5μm, **f** TEM image, 450 nm, **g** FESEM image 1 μm, **h** FESEM image, 250 nm

Changes to endomembrane components during sorbitol acclimatization

Changes to the ultrastructure of endomembrane components were also apparent in cells acclimatized for longer than 24 h. Golgi bodies exhibited distinct in-curling or involution of *trans* face cisternae and the *trans* Golgi network (TGN) became more prominent and increased in size (Fig. 7a). During acclimatization, the processing of EPS in the Golgi body, as exemplified by the formation of large swollen peripheries,

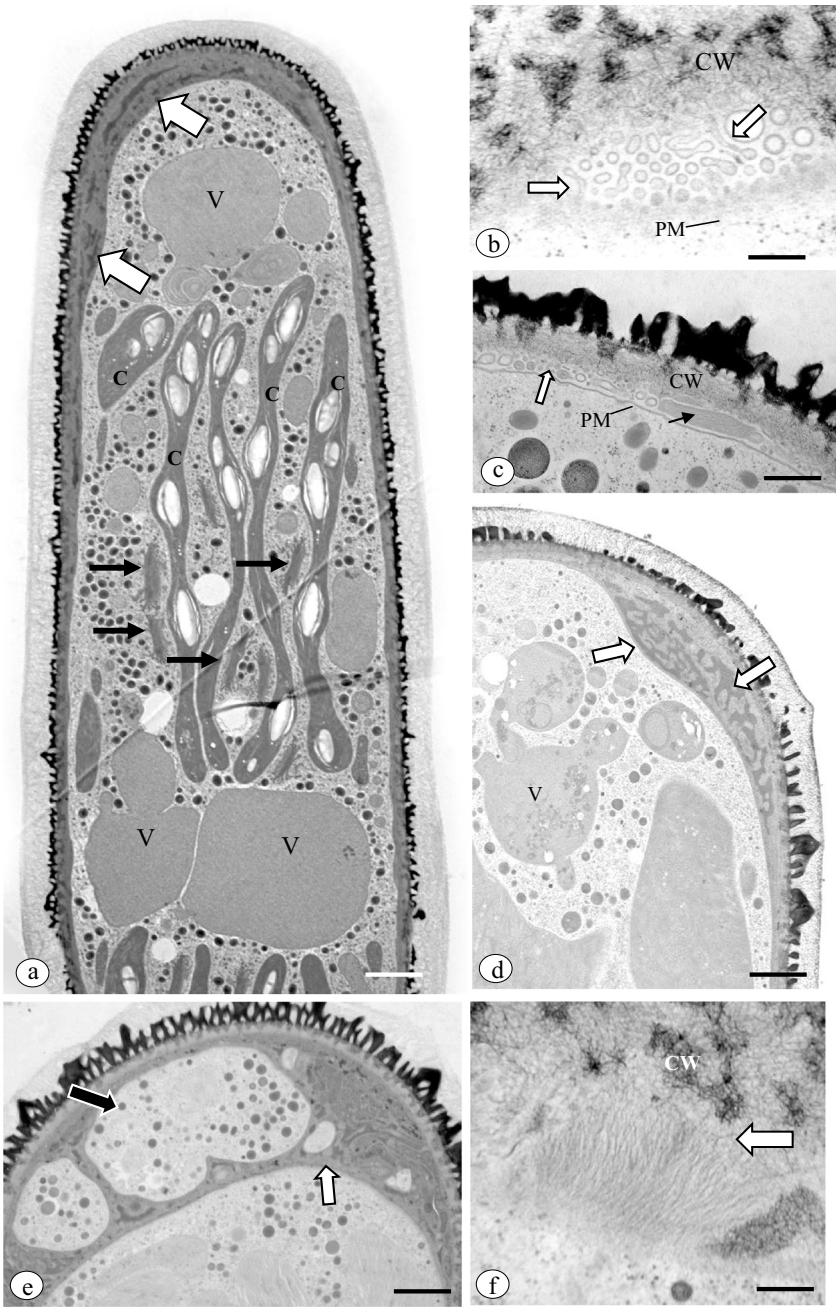

Fig. 5 Peripheral thickenings that form during acclimatization in 200 mM sorbitol. **a** After 24 h of incubation, peripheral thickenings (white arrows) form inside the plasma membrane (PM) at the periphery of the cell. During this time, the positioning of chloroplast lobes (C) and Golgi bodies remain the same as that observed in control cells but large vacuoles (V) appear in the peripheral cytoplasm. **b** During early development of the inclusions (5-240 min), numerous Hechtian strands or remnants thereof are found in inclusions. Note the attachement of these membranous components to the plasma membrane (PM) or inner layer of the cell wall (CW, white arrows). **c** After 24 h or longer, the thickenings contain the strand remnants (white arrow) and a slightly electron dense, homogenous inclusion (black arrow). The plasma membrane (PM) and cell wall (CW) are also apparent. **d** After 72 h, the inclusions (arrows)of the thickenings are found in large branched configurations. The thickening are also notably larger. **e** After 72 h incubation, the thickenings (white arrow) increase in size and are often penetrated by channels of cytoplasm (black arrow). **f** After 72 h incubation, some of the inclusions also conatin bundles of parallel fibrils (arrow). These fibrils appear to extend into the inner layer of the cell wall (CW). All images= TEM. **a** 2.4 μm, **b** 320 nm, **c** 800 nm, **d** 1.7 μm, **e** 1.5 μm, **g** 125 nm

was still apparent (Fig. 7b). Likewise, our observations noted no major alterations to the number of vesicles found in the peripheral cytoplasm. However, acclimatized cells possessed large multi-branched vacuoles just external to the Golgi bodies (Fig. 7c). These vacuoles were more often present at the isthmus and polar zones (Suppl. Fig 1). Many of these vacuoles contained internal membranous components (Suppl. Fig. 3d). Additionally, the cytoplasm was filled with smaller autophagic vacuoles or autophagosomes that contained swirled membrane components and were often penetrated by, or contained, channels of cytoplasm (Fig. 7d). Phagophore-like membranes were also commonly found in these acclimatized cells (Suppl. Fig. 3e, f). During acclimatization, cytokinesis did not occur. The region of the isthmus where cytokinesis typically occurs became filled with small vacuoles, secretory vesicles and Golgi bodies (Fig. 7e).

Acclimatization in polyethylene glycol (PEG) also causes significant alterations

We also assessed acclimatization of cells in another commonly employed osmotic agent, PEG. We initially screened cells incubated in PEG with molecular weights (mw) ranging from 3500, 6000, to 15,000–20,000. Fifteen percent PEG-3,500

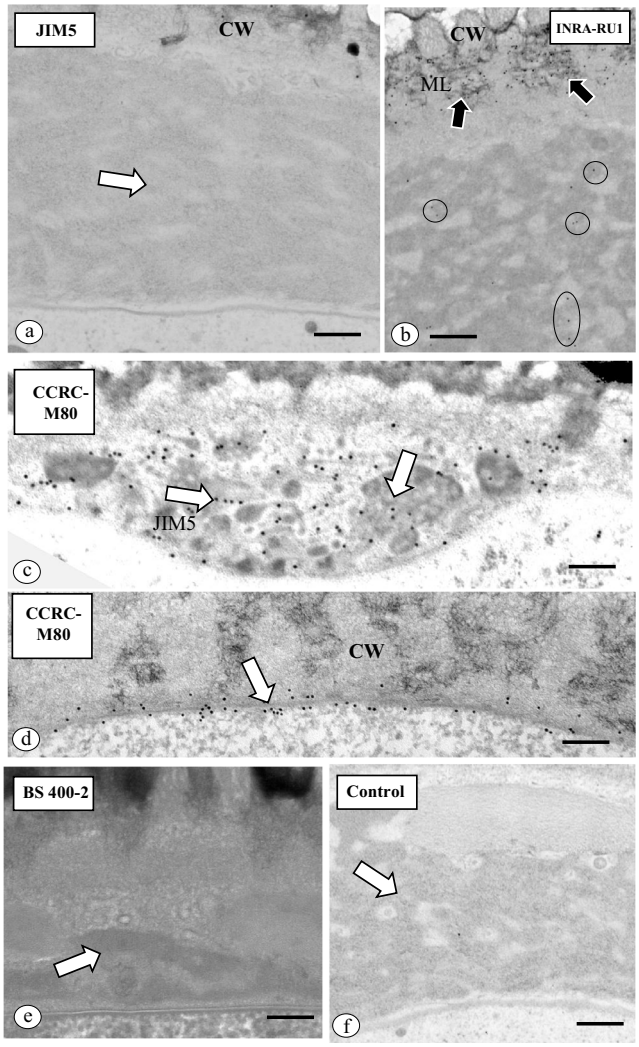

Fig. 6 Immunogold labeling of the peripheral thickenings. JIM5 (**a**) and BS 400-2 (**e**) do not label the components of the thickenings (arrow). (b) INRA-RUI, a mAb that binds to RGI epitopes weakly labels the peripheral thickening (circles) as well as the cell wall (CW) and medial layer (ML, black arrows). **c** The RGI-binding mAb, CCRC-M80, labels the the interior of the thickening (arrows). **d** In control cells, CCRC-M80 labels the interface region between the PM (arrow) and cell wall (CW). **f** Control experiment where primary antibody was excluded shows no labeling (arrow). All images = TEM, **a** 530 nm, **b** 320 nm, **c**. 400 nm , **d** 350 nm, **e** 300 nm, **f** 500 nm

mw PEG was chosen as it produced consistent and relatively rapid results. Cells continued to expand when incubated in 15% PEG-3500 mw in WHS for up to 7 days. After 72 h of incubation, the center of the cell and isthmus zone broadly swelled (Fig. 8a). JIM5-labeling of PEG habituated cells showed that cell expansion still occured but the formation of the HG lattice during acclimatization was much reduced or even absent (Fig. 8b). Like sorbitol acclimatization, there was a 30% +/− 5% increase in new CW surface area than that observed in control cells. When allowed to recover, the HG lattice was produced at the isthmus or expanding pole of dividing daughter cells within 12 h (Figs. 8c, d). TEM analysis of PEG-habituated cells highlighted the loss of the HG lattice (Figs. 8e, f) . Only the inner and medial wall layers were found in altered zones (Fig. 8g). FESEM highlighted the loss of the HG lattice on the wall surface (Fig. 8e).

Discussion

The emergence onto, and successful colonization of, a terrestrial habitat by an ancestor of zygnematophycean algae 500+ mya was a major step in the evolution of land plants and the subsequent transformation of the planet's natural history. The transition from aquatic to terrestrial life required numerous adaptations to counteract new stressors including increased illumination (e.g., light saturation, UV light) and exposure to high concentrations of atmospheric gases (e.g., CO_2, O_2); Furst-Jansen et al. 2020; De Vries and Archiblad, 2018; Delwiche and Cooper 2015, Herburger et al. 2015). Many ancient zygnematophytes, as well as many of their extant progeny, likely lived in shallow freshwater wetlands that experienced periods of drying and consequently, osmotic stress. These algae had to adapt efficiacious structural and physiological mechanisms that allowed them to rapidly respond and acclimatize to osmotic stress over significant periods of time. Recent molecular studies of extant zygnematophytes and other charophytes have shown that the genetic machinery for coping with the challenges of terrestrial life, including osmotic stress and desiccation, were most likely present prior to colonization of terrestrial habitats (Wang et al., 2020b; Jiao et al. 2020; Furst-Jansen et al., 2020; Rensing 2018; Harholt et al. 2016; Holzinger and Karsten 2013). Over the past several decades, Ursula Lütz-Meindl 's and co-workers' elegant studies of the cellular, biochemical and ecophysiological mechanisms for responding to various stressors in zygnematophytes have similarly provided valuable insight into acclimatization strategies of these algae (Lütz-Meindl 2016). Recent investigations of land plant cell acclimatization to osmotic and other abiotic stressors have clearly shown that stress sensing and initiation of signal transduction networks for stress response are often focused at the CW and PM (Rui and Dinneny, 2020; Novakovic et al. 2018; Wang et al. 2016: Tenhaken 2015). Presently, we are only just beginning to elucidate CW/PM responses to abiotic stress in zygnematophytes (Jiao et al. 2020; Herburger et al. 2019). This study highlights key subcellular events that occur in response to osmotic stress in the model zygnematophyte, *Penium*.

General observations

Sorbitol incubation was chosen as the main experimental agent for inducing osmotic stress. It is non-toxic and "versatile" in that it was most effective for observing Hechtian strands when used at 300 mM concentration and for

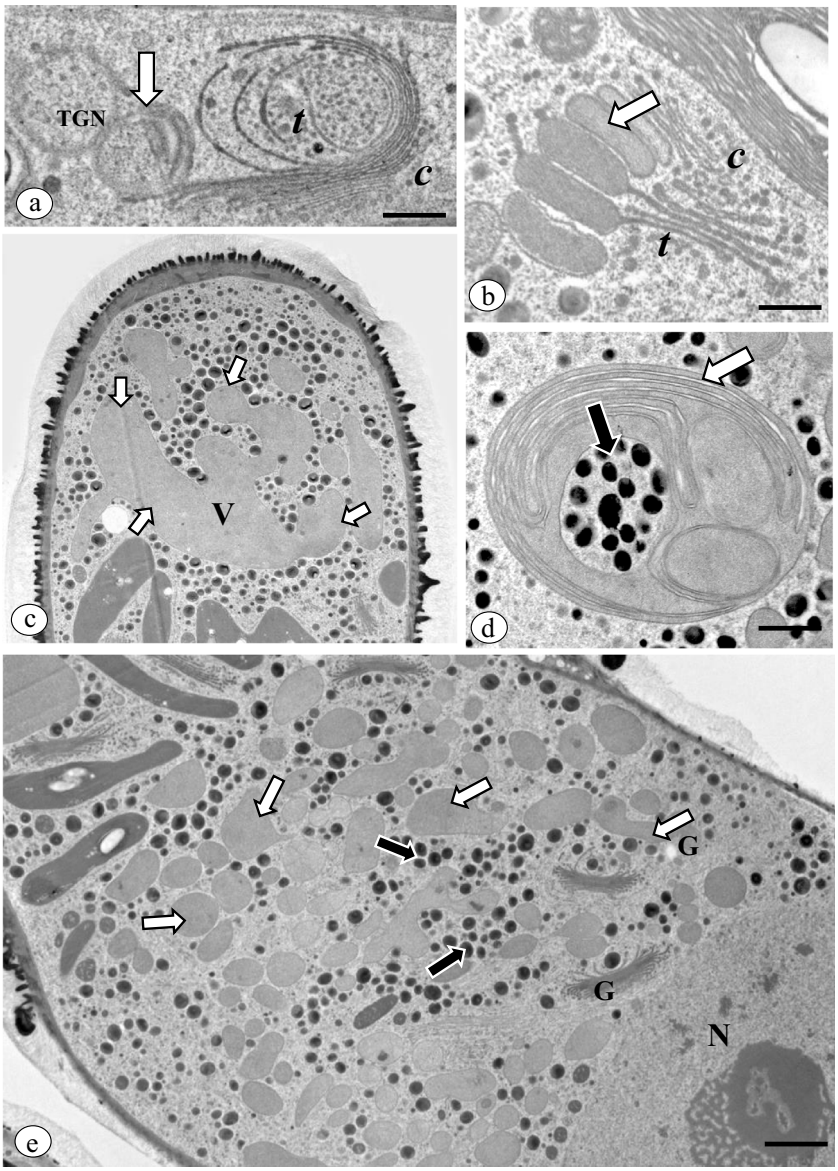

Fig. 7 Subcellular changes that occur during acclimatization. **a** After 24 h of incubation, Golgi body cisternae displayed notable involution or incurling at the trans face (*t*). The trans Golgi network (TGN, arrow) is larger and more pronounced in treated cells. The cis (*c*) face is apparent. **b** During sorbitol acclimatization (24 h), Golgi bodies still produce extracellular polymeric substance (EPS) materials as exemplified by the production of large swollen peripheries of the cisternae (arrow). The cis (*c*) and trans (*t*) faces are also apparent. **c** The peripheral cytoplasm during acclimatization (24 h) contains large branched vacuoles (V, arrows). **d** Additionally, distinct vacuoles, most likely autophagic vacuoles or autophagosomes (white arrow) are commonly found in the cytoplasm after 24 h of treatment. Cytoplasm penetrates or is included in these vacuoles (black arrow). **e** Cytokinesis does not occur during axcclimatization. In the zone where the cytokinetic apparatus is normally found, the cytoplasm becomes filled with secretory vesicles (white arrows), small vacuoles (black arrows) and Golgi bodies (G). All images= TEM, **a** 500 nm, **b** 625 nm, **c** 2.8 μm, **d 120** nm, **e** 1.5 μm

monitoring acclimatization events in cells over for up to 7 d at lower concentrations (200 mM). For the latter, the major effects of sorbitol treatment (e.g., peripheral thickenings, changes to vacuoles, appearance of autophagy compartments) appeared at 24 h and increased incrementally for up to 7 days (e.g., larger vacuoles, increased size of peripheral thickenings). After 7 days, cells entered into a senescence phase. The concentration of sorbitol needed to induce cellular changes in *Penium* was much lower than that required for field collected samples (Kaplan et al., 2012a, b). Determination as to whether this was simply a unique feature of log phase laboratory cultures or if it represents an actual higher sensitivity of *Penium* to osmotic stress is not yet known. TEM imaging was chosen as the main microscopy tool as the unicellular *Penium* is conveniently fixed for TEM via spray freezing-based cryofixation and freeze substitution. This allowed for the rapid screening of a large set of treated cells that yield "snapshots" of key acclimatization events. We also incubated cells in PEG, an agent commonly used for simulating osmotic stress in plants (Ji et al. 2014; Lang et al. 2014; Rao and FTZ, 2013), in order to compare its acclimatization responses with those obtained with sorbitol. As with sorbitol treatment, PEG acclimatization transforms the architecture of the CW, inhibits cytokinesis and yields elongate cells. For both, expansion rates based on CW surface area covered by new HG lattice (Domozych et al. 2009) are notably greater than that of control cells. Unlike treatment with sorbitol, PEG treatment does not result in the formation of Hechtian strands or at least ones that were stable enough to allow for TEM processing. Likewise, PEG acclimatization results in the swelling of cells at the cell center versus the production of a highly irregular CW observed during sorbitol treatment. No peripheral thickenings

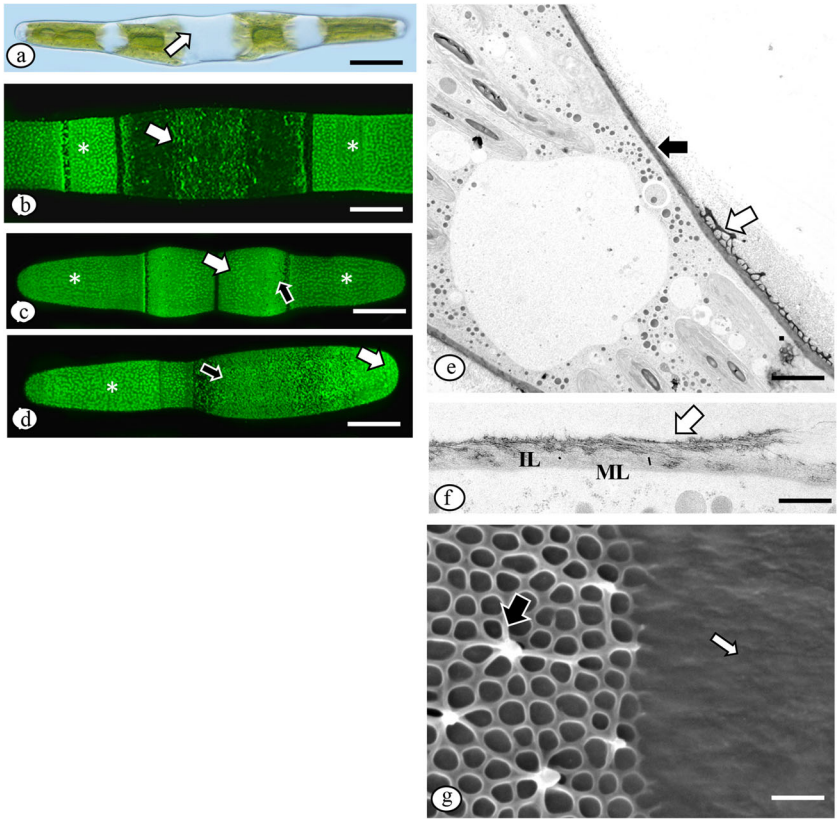

Fig. 8 Acclimatization effects of PEG (mw 3,500) and NaCl. **a** Cell habituated for 72 h in PEG exhibiting swollen cell center (arrow). **b** JIM5-labeling of a cell incubated for 48 h in PEG reveals the weak labeling at the swollen central zone of the cell (arrow). The CW formed before incubation contains the distinct HG lattice (*) of the outer CW. **c** Recovery of HG lattice (white arrow) at the isthmus. The altered CW formed during PEG treatment (black arrow) and the CW formed before PEG incubation (*) are also noted. **d** Recovery of HG lattice (white arrow) at the isthmus. d Recovery of the HG lattice at the tip of the pole a daughter cell just after cell division. The altered CW formed during PEG treatment (black arrow) and the CW formed before PEG incubation (*) are also noted. **e** TEM image of transition zone between pre-existing CW (white arrow) and the CW formed during PEG treatment (black arrow). The lattice is missing from the altered CW. **f** Magnified view of the altered CW of a PEG-treated cell. Note that while the HG lattice is missing (white arrow) but the medial (ML) and inner (IL) layers are present. **g** FESEM image of the interface of altered and pre-existing CW in cell habituated in PEG. Note the absence of the lattice (white arrow) in the altered CW versus the pre-existing wall (black arrow) that contains the lattice. **a** DIC image, 35 μm, **b** CLSM image, 11.4 μm, **c** CLSM image, 17 μm, **d** CLSM image 12.5 μm, **e** TEM image, 4.5 μm, **f** TEM image, 2.6 μm, **g** FESEM image, 2.2 μm

are observed, the Golgi bodies show little if any structural change and few if any of the large vacuoles (e.g., peripheral vacuoles) or autophagic vacuoles are observed with PEG treatments. Significant differences in response to sorbitol versus PEG treatment are not surprising and have been well documented in plants (Osmolovskaya et al. 2018; Slama et al. 2007; Hsu and Kao 2003; Shao et al. 2015). Sugar alcohols like sorbitol readily penetrate the cell and become involved in cell metabolism while PEG does not penetrate and is inert. These features most likely account for the differences in response between sorbitol and PEG in *Penium*.

Hectian strands

The physiology of osmotic stress has been a major subject of interest in plants especially for agriculturally important taxa that live in habitats that experience low water conditions. Recent molecular dissection of stress-induced plant cells has significantly enhanced our understanding of the cell, tissue, and organ response mechanisms and acclimatization strategies to this stress (Gupta et al. 2020; Feng et al. 2016). Cell biology-based investigations have demonstrated that in many plant cells, microzones of the PM strongly adhere to the CW during plasmolysis caused by osmotic stress. This results in the formation of thin connections or Hechtian strands (Hecht 1912; Yoneda et al. 2020) between the CW and PM that range in size between 30 and 250 nm in diameter (Cheng et al. 2017; Baluska et al. 2003). The function of Hechtian strands remains incompletely resolved (Liu et al. 2015; Buer et al. 2000; Pont-Lezica et al. 1993). It has been suggested that they serve as a reservoir of PM during plasmolysis and during de-plasmolysis, they provide an orderly restoration of cell and PM function. The strands may also play a role in the maintenance of cell polarity by limiting slippage of the cytoplasm against the CW. The connection points of the strands to specific loci of the CW may also serve as a means for certain PM proteins to retain their location along the cell surface.

Penium rapidly forms Hechtian strands upon exposure to sorbitol-based osmotic stress and plasmolysis of the protoplast. Within 1 min of incubation in 300 mM sorbitol, plasmolysis begins and the protoplast initiates retraction from the CW. Hechtian strands appear and elongate upon further shrinkage of the protoplast. Subsequently, the space between the protoplast and CW fill with an estimated 1000–1500 Hechtian strands. The strands emerge at approximately 300 nm intervals off the PM and in an ordered pattern. While Hecthian strands in many plant cells are associated with ER or cytoskeletal components (Cheng et al. 2017), there was little evidence for. ER, actin filaments or microtubules in the strands of *Penium*, an observation also noted in a previous study of the zygnematophyte, *Closterium acerosum* (Domozych et al. 2003). In another zygnematophyte, *Zygnema*, osmotic stress-induced vesicular structures were also found in periplasmic spaces (i.e., very likely remnants of these strands) and they also did not contain cytoskeletal elements (Kaplan et al. 2012b). The absence of ER and cytoskeletal components in the Hechtian strands of zygnematiophytes may be a result of their high lability during plasmolysis. Further analysis will be required to resolve this.

What are the possible functional roles of Hechtian strands in *Penium*? The attachment of specific PM zones to the CW is the basis of strand formation. This attachment in higher plants has been thought to be mediated by various proteins including GPI (glycosylphosphatidylinositol)-anchored proteins, integrin-like proteins, receptor-like kinases, wall associated kinases and arabinogalactan proteins or AGPs (Lopez-Hernandez et al. 2020; Liu et al. 2015; Tenhaken 2015; Lang et al. 2014, 2004). These proteins function as CW integrity (CWI) sensors that recognize changes in the mechanical properties of the CW. CWI sensors and signal recptors located at the PM transduce signals and send them into the cytoplasm to initiate changes in the CW in order to maintain integrity and cellular function (Novakovic et al. 2018). Some CWI sensors are also involved in the cell's secretory apparatus (e.g., vesicle-PM recognition and fusion events) and CW deposition/biosynthesis (Liu et al. 2015; Baluska et al. 2003). Recent studies (Lopez-Hernandez et al. 2020; Lamport et al., 2018) have also interpreted the components of Hechtian strand adhesion zones at the CW to be force transducers that couple internal stress in growing CWs to the PM. The strands are associated with CW AGP and form a type of "capacitor" that effects cytosolic Ca^{2+} oscillations that in turn, control CW polymer secretion and polymer incorporation in the CW. Palacio-Lopez et al. (2020) recently demonstrated that AGP is a component of the *Penium* CW and is found in thin fibrils coating the outer HG lattice of the CW. The major function of this AGP is cell adhesion. However, the presence of the AGP-fibrils over the entire CW surface suggests that they may have a mechanosensory role as well. For example, *Penium* is often found in shallow wetlands that frequently experience considerable evaporation during summer periods. In laboratory experiments that mimic low water conditions conditions of these wetlands (Jiao et al. 2020), *Penium* secretes large amounts of a polysaccharide-based EPS or mucilage. This hygroscopic material encoats the cell most likely as a way to retain water during drying periods as well as for "fueling" the cell's gliding mechanism (Domozych et al. 2020, Palacio-Lopez et al. 2019). EPS is synthesized in the Golgi Apparatus and transported to the peripheral cytoplasm in large vesicles. These vesicles circulate around the cell via actin-mediated cytoplasmic streaming. That is, a ready supply of EPS constantly circulates just under the PM. The release of EPS (i.e., fusion of EPS vesicles with the PM) from the cell can occur at any point of the cell surface in response to specific external signals. If *Penium* makes contact with a substrate and adheres to it via its AGP fibrils, an associated mechanism may also be triggered to activate EPS secretion at certain surface loci in order to encoat the cells with EPS or to "fuel" the gliding of the cell to particular sites on a substrate (Domozych et al. 2020). These localized secretion events would require the rapid activation of specific EPS vesicle-fusion sites on the PM at particular zones of the cell surface. The large number of CW-PM adhesion sites identified by Hectian strand formation may represent *Penium*'s complex "circuitry" of specific protein aggregates that facilitate EPS vesicle fusion with the PM. The AGP fibrils on the CW surface may be the initial signal receptors that initiate a communication conduit through the CW to these specific PM sites. We might posit then that the AGP fibrils on the CW surface "sense" osmotic stress. A signal is then sent through the CW to these special PM sites that then activate EPS vesicle-PM binding/tethering that in turn, facilitates EPS vesicle fusion with the PM and the subsequent extrusion of this mucilage through the CW. Alternatively, the PM-CW adhesion sites may serve as structural braces that stabilize PM association with the CW during rapid EPS secretion (i.e., the vesicle fusion sites are at zones not marked by the CW-PM adhesion zones). For example, during initial plasmolysis in *Closterium acerosum*, TEM imaging shows that PM-CW adhesion sites of the PM to the CW during early Hechtian strand formation are positioned next to but not at the pores that decorate the CW (Domozych et al. 2003). These pores are the sites for the extracellular release of EPS. *Penium* does not possess CW pores but secretes EPS directy through its CW. The resolution of the components of the PM-CW adhesion sites and their functional roles in EPS secretion *Penium* await further study.

The CW and cell shape are altered by acclimatization to osmotic stress

Penium margaritaceum possesses a distinct Ca^{2+}-complexed HG lattice in the outer layer of its CW (Palacio-Lopez et al. 2020, Domozych et al., 2014, 2007). During an

acclimatization period while in sorbitol- or PEG-containing growth medium, significant changes to the HG lattice occur. Sorbitol treatment results in a transformation of the lattice into an irregular series or patches of HG fibers on the CW surface and the absence of the typical lattice projections. PEG treatment results in a complete loss of all components of the HG lattice. These changes to the CW architcture complement the growing pool of evidence that highlights the structural and biochemical alterations to the CW caused by abiotic stress exposure in land plants (Vaahtera et al. 2019; Novakovic et al. 2018; Wang et al. 2016: Tenhaken 2015) as well as in charophytes (Palacio-Lopez et al. 2020; Herburger et al., 2019, 2018, 2015; Lütz-Meindl 2016). In charophytes, these include changes to the structure/function of pectins (Palacio-Lopez et al. 2020; Herburger et al. 2019; Domozych et al. 2014), cellulose (Ochs et al. 2014), noncellulosic polysaccharides (i.e., NCPs, e.g. hemicelluloses; Herburger et al. 2018), and other CW components (Lütz-Meindl 2016) including ß1-3 glucans (i.e., callose; Herburger and Holzinger 2015). In *Penium*, the HG lattice alterations are accompanied by changes to cell shape, an increase in cell expansion rates and a cessation of cytokinesis. Removal of the entire HG lattice by PEG incubation results in a general swelling at the isthmus while the incomplete removal of the lattice by sorbitol incubation causes little or no swelling but irregular shape changes at the isthmus. In both osmotic agents, the cells maintain a general cylindrical shape. These observations indicate that the HG lattice is not the primary architectural component of the CW that maintains the cylindrical cell shape. Previous work (Palacio-Lopez et al. 2020) has demonstrated that most chemical and enzymatic treatments that compromise the HG lattice do not the affect general cylindrical cell shape. However, incubation of cells in the microtubule-affecting agents, oryzalin and APM, that most likely affect cellulose microfibril formation at the isthmus, cause significant swelling leading to the mainfestaion of a spherical shape at the isthmus (Palacio-Lopez et al. 2020; Domozych et al., 2014). These observations indicate that the inner cellulosic layer of the CW of *Penium* is the primary shape-maintaining structural component of the CW. However, the results of our study also suggest that the HG lattice may contribute secondarily to maintaining cell shape. When fully formed in untreated cells, the lattice consists of branched, interlocking Ca^{2+}-complexed HG fibers that cover the entire CW surface. If the lattice is completely removed from the expanding CW as in PEG-induced osmotic stress, the inner cellulosic layer maintains the general cylindrical shape. However, the absence of the interlocking fiber-network of the HG lattice contributes to some of the CW's structural resistance to internal turgor pressure during expansion and results in a general swelling at the isthmus. When incubated in sorbitol-containing medium, the partially formed HG lattice results in CW zones of varying rigidity and expansion resistance. Those areas that have interlocking lattice components maintain CW resistance to internal pressure but surrounding lattice-free zones do not and yield to the pressure. This results in the irregular CW structure and cell shape at the isthmus. Alternatively, it has been recently shown (Haas et al. 2020; Zhang and Zhang 2020) that CW expansion may be a function of pectin nanofibril dynamics (e.g., methylation state) and not of a turgor-driven mechanism. Perturbation of this nanofibril behavior by osmotic stress in *Penium* may result in disruption of normal CW polymer interactions at the CW expansion zone and the subsequent changes to CW and cell shape.

This study also reveals that during acclimatization in osmotic agents, cell expansion is notably greater than that observed in control cells and cytokinesis ceases. We estimate that cells incubated in 200 mM sorbitol for 24, 48, and 72 h had approximately 30% more new CW surface area than that seen in control cells. This leads to highly elongate cells that, in the case of sorbitol-treated cells, results in a "filamentous" phenotype. In most plant cells and tissues, osmotic stress initially stops or reduces expansion (Rui and Dinneny, 2020; Novakovic et al. 2018) but after an acclimatization period, expansion returns. In *Penium*, we noted that the increased rate of expansion in sorbitol- and PEG-treated cells begins within 24 h of incubation and therefore shows that acclimatization to osmotic stress occurs much more rapidly than that observed in land plants. *Penium*'s response to osmotic stress most likely includes both resumption of its CW biosynthesis/secretion apparatus in order to continue expansion as well as a cessation of cytokinesis, a phenomenon that has also been demonstrated in plants during periods of abiotic stress (Tang et al 2011). The resulting filamentous phenotype exhibited in *Penium* may constitute an effective means of increasing CW surface area that subsequently enhances absorption of water. For example, in cells at the edge of a shallow wetland that is experiencing drying, the formation of the elongate phenotype would increase the chances of maintaining at least part of the CW in water that can then be absorbed to maintain normal cell functioning (anti-plasmolysis response).

Sorbitol acclimatization and the formation of peripheral thickenings

During acclimatization, distinct peripheral thickenings are formed between the CW and PM. During short-term incubation in sorbitol, the thickenings consist of an invagination of the PM that contain membranous components. Some are attached to the PM or CW. We interpret these membranes as Hechtian strands or remnants thereof. After longer acclimatization periods, the thickenings expand throughout the cell periphery and in some cases, are penetrated by cytoplasm. These thickenings also contain membranous components that may include remnants of Hechtian strands. However, some membrane profiles also resemble paramural vesicles that are

found in the appositions or papillae in the peripheries of plant cells when under fungal pathogen attack (Li et al. 2018; An and van Bel, 2007, An et al., 2006). Likewise, aggregations of vesicles or "multivesicular" compartments between the PM and CW have been described in plant cells not under stress. These have been postulated to be a an exocyst-like or -based release of autophagous membrane components outside the PM as a means to remove excess membrane from the cell (Cui et al. 2020; Zhang et al. 2019; Overdijk et al., 2020; Pecenková et al. 2018, Lin et al. 2015). In this study, we also describe multiple autophagous components that appear at the same time as the thickenings (see later). It is possible that these peripheral thickenings may be products of a hyper-expulsion mechanism of autophagous membranous components that form during acclimatization to osmotic stress.

These thickenings also contain a branched granular matrix that is moderately osmiophilic. These are similar in appearance to the constituents of CW appositions found in various plant cells that have been shown to contain CW components like callose, proteins, inorganic materials and lignin (Collinge, 2009; LeRoux et al., 2011). Our immunogold labeling of the *Penium* thickenings demonstrate that they do not contain HG, xyloglucan, xylan, AGP or callose and our labeling with Calcofluor show that they do not contain cellulose (data not shown). However, two RG-I binding mAbs, CCRC-M80 and INRA-RU1 do label the thickenings. In control cells, CCRC-M80 labels the interface of the CW and PM and in sorbitol acclimated cells, the mAb labels the thickenings. INRA-RU1 labels the medial layer of the CW and also weakly labels the thickenings. The different levels of labeling are most likely due to different epitope recognition by the mAbs. However, this labeling shows that RG-I is a constituent of the thickenings. In a previous study (Domozych et al. 2014), RG-I was also shown to be located in the medial CW layer of *Penium* and is connected to/anchors the the HG lattice of the outer CW layer. During cell expansion, RG-I is also incorporated into the CW architecture prior to the deposition and formation of the HG lattice. How then might the presence of RG-I in the thickenings be explained? It is possible that during sorbitol acclimatization, as PM pulls away from the CW, RG-I is released from the PM and into the spaces that will contain the peripheral thickenings (i.e., not the CW). The lack of RG-I in the expanding CW would then alter deposition and incorporation of the HG and result in the irregular lattice.. Another possibility is that the reduction of turgor pressure restricts or inhibits recycling of CW precursors at the CW expansion zone that are, in turn, deposited in the space between the PM and CW. Our results add to the growing pool of data that show pectins being directly affected by abiotic stress (Yang et al. 2020; Bilska-Kos et al. 2017).

The granular matrix of the peripheral thickenings most likely contains other biochemical consituents such as osmolytes. Osmotic stress is known to trigger the biosynthesis and accumulation of osmolytes in plants and green algae (Holzinger and Karsten, 2013). It is likely that the production of osmolytes during osmotic stress must be regulated and their release to the peripheral thinckening may be a manifestation maintaining a critical balance..

Sorbitol treatment causes changes to the endomembrane system

The endomembrane system of plants has been shown to modulate both structurally and functionally in response to abiotic stress (Wang et al. 2020b). Central to the processing (i.e., synthesis, packaging and transport to the cell surface) of the CW and other extracellular matrix components is the Golgi Apparatus. *Penium*'s Golgi Apparatus is composed of 125–150 Golgi bodies per cell that are are positioned in disitnct linear arrays in cytoplasmic valleys and are responsible for processing CW and EPS components (Domozych et al. 2020). When acclimatized to sorbitol-induced osmotic stress, the Golgi bodies display notable in-curling or involution of the *trans* face cisternae and the increased appearance of TGN components. However, the presence of swollen cisternal peripheries (i.e., precursors to EPS vesicles) and the enhanced expansion of the CW during acclimatization indicates that the Golgi Apparatus still functions. Likewise, our observations did not reveal any notable changes to vesicle number in the cell periphery or changes to EPS secretion. The HG lattice though was significantly altered during acclimatization to osmotic stress and may be indicative of both quantitative and qualitative alterations to the pectin processing machinery in the secretory membrane trafficking network. That is, a decreased level of HG processed by the Golgi Apparatus and/or changes to HG chemistry during processing may be responsible for the production of the altered HG lattice during sorbitol treatment or the absence of the lattice during PEG treatment. Recent mining of *Penium*'s genome (Jiao et al. 2020) has revealed a very large number of pectin processing/modulating genes and further investigation of specific pectin gene(s) expression during acclimatization should provide significant insight into CW polymer responses to abitotic stress.

Sorbitol acclimatization results in transformation of the cell's vacuolar components. First, after 24 h or longer incubation, smaller autophagic vacuoles or autophagophores along with phagophore-like membranous components appear in the cytoplasm. Second, the network of large vacuoles that reside in the peripheral cytoplasm (see Domozych et al. 2020) increase in size and branching. During longer incubation periods, these vacuoles contain various membranous constituents. We interpret these vacuolar changes as being manifestations of macroautophagy that is commonly observed in plants and other eukaryotes (Qi et al. 2020; Zeng et al. 2019; Ding et al. 2018; van Doorn and Papini 2013). It is likely that long incubation periods of cells under osmotic stress conditions

may signal the onset of programmed cell death, i.e., a developmental event often accompanied vacuolar changes and macroautophagy (Zheng et al. 2019; Affenzeller et al. 2009a, b). Autophagy is a process that sends damaged organelles to the vacuole for degradation or storage and is activated during abiotic stress and/or as part of programmed cell death. Autophagy is the cell's way of maintaining homeostasis via controlled recycling. It is also a mechanism that regulates sugar and other nutrient levels in plant cells (van Rensburg et al. 2019; Masclaux-Daubresse et al. 2017). Our results with *Penium* indicate that sorbitol-induced stress activates the autophagy network and may be a response for acclimatizing the the input of large amounts of a sugar alcohol.

Conclusion

Acclimatization to osmotic stress results in multiple and significant alterations to the CW-PM domains and endomembrane system of *Penium*. This includes production of Hechtian strands, changes to CW architecture and cell shape, the formation of distinct peripheral thickenings and alterations to endomembrane components of the cell. These subcellular modulations most likely were important mechanisms that ancient zygnematophytes employed when colonizing land.

Supplementary Information The online version contains supplementary material available at https://doi.org/10.1007/s00709-021-01644-y.

Acknowledgements The authors dedicate this paper to Professor Ursula Lütz-Meindl whose outstanding research career provided keen insight into zygnematophyte biology and who was a true inspiration to colleagues and students. The authors also thank the US-National Science Foundation (NSF; NSF-MCB 1517345) for support of this project.

Author contribution All aurhors participated in experimental and data gathering activities. All authors contributed to writing this manuscript.

Funding This work was funded by the National Science Foundation (USA) grant: MCB-1517546.

Data availability All data and material available upon request.

Declarations

Ethics approval All ethics guidelines have been followed.

Consent to participate All authors agree to participate in this manuscript preparation and review.

Consent for publication All authors agree to the publication this article if accepted.

Conflict of interest The authors declare no competing interests.

References

Abdul Malik NA, Kumar IS, Nadarajah K (2020) Elicitor and receptor molecules: orchestrators of plant defense and immunity. Int J Mol Sci 21:963. https://doi.org/10.3390/ijms21030963

Affenzeller MJ, Darehshouri A, Andosch A, Lütz C, Lütz-Meindl U (2009a) PCD and autophagy in the unicellular green alga Micrasterias denticulata. Autophagy 5:854–855. https://doi.org/10.4161/auto.8791

Affenzeller MJ, Darehshouri A, Andosch A, Lütz C, Lütz-Meindl U (2009b) Salt stress-induced cell death in the unicellular green alga *Micrasterias denticulata*. J Exp Bot 60:939–954. https://doi.org/10.1093/jxb/ern348

Ali O, Traas J (2016) Force Driven Polymerization and Turgor-Induced Wall Expansion. Trends Plant Sci 21:398–409. https://doi.org/10.1016/j.tplants.2016.01.019

An Q, Huckelhoven R, Kogel K-G, van Bel AJE (2006) Multivesicular bodies participate in a cell wall-associated defence response in barley leaves attacked by pathogenic powdery mildew fungus. Cell Microbiol 8:1009–1019. https://doi.org/10.1111/j.1462-5822.2006.00683.x

An Q, van Bel AJ, Hückelhoven R (2007) Do plant cells secrete exosomes derived from multivesicular bodies? Plant Signal Behav 2:4–7. https://doi.org/10.4161/psb.2.1.3596

Baluska F, Samaj J, Wojtaszek P, Volkmann D, Menzel D (2003) Cytoskeleton-Plasma Membrane-Cell Wall Continuum in Plants. Emerging Links Revisted. Plant Physiol 133:482–491. https://doi.org/10.1104/pp.103.027250

Bashline L, Lei L, Li S, Gu Y (2014) Cell Wall, Cytoskeleton, and Cell Expansion in Higher Plants. Mol Plant 7:586–600. https://doi.org/10.1093/mp/ssu018

Becker B, Feng X, Yin Y, Holzinger A (2020) Desiccation tolerance in streptophyte algae and the algae to land plant transition: evolution of LEA and MIP protein families within the Viridiplantae. J Exp Bot 71:3270–3278. https://doi.org/10.1093/jxb/eraa105

Bidhendi AJ, Geitmann A (2018) Finite Element Modeling of Shape Changes in Plant Cells. Plant Physiol 176:41–56. https://doi.org/10.1104/pp.17.01684

Bilska-Kos A, Solecka D, Dziewulska A, Ochodzki P, Jończyk M, Bilski SP (2017) Low temperature caused modifications in the arrangement of cell wall pectins due to changes of osmotic potential of cells of maize leaves (Zea mays L.). Protoplasma 254:713–724. https://doi.org/10.1007/s00709-016-0982-y

Buer CS, Weathers PJ, Swartzlander GA (2000) Changes in Hechtian Strands in Cold-Hardened Cells Measured by Optical Microsurgery. Plant Physiol 122:1365–1377. https://doi.org/10.1104/pp.122.4.1365

Buschmann H, Holzinger A (2020) Understanding the algae to land plant transition. J Exp Bot 71:3241–3246. https://doi.org/10.1093/jxb/eraa196

Cheng X, Lang I, Opeyemi O, Griffing L (2017) Plasmolysis-deplasmolysis causes changes in endoplasmic reticulum form, movement, flow, and cytoskeletal association. J Exp Bot 68:4075–4087. https://doi.org/10.1093/jxb/erx243

Collinge DB (2009) Cell wall appositions: the first line of defence. J Exp Bot 60:351–352. https://doi.org/10.1093/jxb/erp001

Cosgrove DJ (2016) Plant cell wall extensibility: connecting plant cell growth with cell wall structure, mechanics, and the action of wall-modifying enzymes. J Exp Bot 67:463–476. https://doi.org/10.1093/jxb/erv511

Cosgrove DJ (2018) Diffuse Growth of Plant Cell Walls. Plant Physiol 176:16–27. https://doi.org/10.1104/pp.17.01541

Cui Y, Gao J, He Y, Jiang L (2020) Plant extracellular vesicles. Protoplasma 257:3–12. https://doi.org/10.1007/s00709-019-01435-6

Davis DJ, Wang M, Sørensen I, Rose JKC, Domozych DS, Drakakaki G (2020) Callose deposition is essential for the completion of cytokinesis in the unicellular alga, Penium margaritaceum. J Cell Sci 133: jcs249599. https://doi.org/10.1242/jcs.249599

De Vries J, Archiblad JM (2018) Plant evolution: landmarks on the path to terrestrial life. New Phytol 217:1428–1434. https://doi.org/10.1111/nph.14975

De Vries J, Curtis BA, Gould SB, Archiblad JM (2018) Embryophyte stress signaling in the algal progenitos of land plants. PNAS 115: E3471–E3480. https://doi.org/10.1073/pnas.1719230115

Dehors J, Mareck A, Kiefer-Meyer M-C, Menu-Bouaouiche L, Lehner MJ-C (2019) Evolution of Cell Wall Polyemrs in Tip-Growing Lnad Plant Gametophytes: Composition, Distribution, Functional Aspects and Their Remodeling. Front Plant Sci 10:441. https://doi.org/10.3389/fpls.2019.00441

Delwiche CF, Cooper ED (2015) The Evolutionary Origin of a Terrestrial Flora. Curr Biol 25:R899–R910. https://doi.org/10.1016/j.cub.2015.08.029

Ding X, Zhang X, Otegui MS (2018) Plant autophagy: new flavors on the menu. Curr Opin Plant Biol 46:113–121. https://doi.org/10.1016/j.pbi.2018.09.004

Domozych DS, Roberts R, Danyow C, Flitter R, Smith B (2003) Plasmolysis, Hechtian strand formation, and localized membrane wall adhesions in the desmid *Closterium acerosum* (Chlorophyta). J Phycol 39:1194–1206. https://doi.org/10.1111/j.0022-3646.2003.03-033.x

Domozych DS, Serfis A, Kiemle SN, Gretz MR (2007) The structure and biochemistry of charophycean cell walls: I. Pectins of Penium margaritaceum. Protoplasma 230:99–115. https://doi.org/10.1007/s00709-006-0197-8

Domozych DS, Lambiasse L, Kiemle S, Gretz MR (2009) Cell Wall Development and Bipolar Growth In The Desmid *Penium Margaritaceum* (Zygnematophyceae, Streptophyta). Asymmetry In An Asymmetric World. J Phycol 45:879–893. https://doi.org/10.1111/j.1529-8817.2009.00713.x

Domozych DS, Fuijimoto C, LaRue T (2013) Polar Expansion Dynamics in the Plant Kingdom: A Diverse and MultifunctionalJourney on the Path to Pollen Tubes. Plants 2:148–173. https://doi.org/10.3390/plants2010148

Domozych DS, Sørensen I, Popper ZA, Ochs J, Andreas A, Fangel JU, Pielach A, Sacks C, Brechka H, Ruisi-Besares P, Willats WGT, Rose JKC (2014) Pectin metabolism and assembly in the cell wall of the charophyte green alga *Penium margaritaceum*. Plant Physiol 165:105–118. https://doi.org/10.1104/pp.114.236257

Domozych DS, Sun L, Palacio-Lopez K, Reed R, Jeon S, Li M, Jiao C, Sørensen FZ, Rose JKC (2020) Endomembrane architecture and dynamics during secretion of the extracellular matrix of the unicellular charophyte, *Penium margaritaceum*. J Expt Bot 71:3323–3339. https://doi.org/10.1093/jxb/eraa039

Feng W, Lindner H, Robbins NE, Dinneny JR (2016) Growing Out of Stress: The Role of Cell- and Organ-Scale Growth Control in Plant Water-Stress Responses. Plant Cell 28:1769–1782. https://doi.org/10.1105/tpc.16.00182

Furst-Jansen JMR, de Vries S, de Vries J (2020) Evo-physio: on stress responses and the earliest land plants. J Exp Bot 71:3254–3269. https://doi.org/10.1093/jxb/eraa007

Gupta A, Rico-Medina A, Cano-Delgado AI (2020) The physiology of plant responses to drought. Science 368:266–269. https://doi.org/10.1126/science.aaz7614

Haas KT, Wightman R, Meyerowitz EM, Peaucelle A (2020) Pectin homogalacturoan nanofilament expansion drives morphogenesis in plant epidermal cells. Science 367:1003–1007. https://doi.org/10.1126/science.aaz5103

Harholt J, Moestrup Ø, Ulvskov P (2016) Why plants were terrestrial from the beginning. Trends Plant Sci 21:96–101. https://doi.org/10.1016/j.tplants.2015.11.010

Hecht K (1912) Studien uber den Vorang der Plasmolyse. Beitr Biol Pflanz 11:137–192

Herburger K, Holzinger A (2015) Localization and quantification of callose in the streptophyte green algae *Zygnema* and *Klebsormidium*: correlation with desiccation tolerance. Plant Cell Physiol 56:2259–2270. https://doi.org/10.1093/pcp/pcv139

Herburger K, Lewis LA, Holzinger A (2015) Photosynthetic efficiency, desiccation tolerance and ultrastructure in two phylogenetically distinct strains of alpine *Zygnema* sp. (Zygnematophyceae, Streptophyta): role of pre-akinete formation. Protoplasma 252: 571–589. https://doi.org/10.1007/s00709-014-0703-3

Herburger K, Ryan LM, Popper ZA, Holzinger A (2018) Localisation and substrate specificities of transglycanases in charophyte algae relate to development and morphology. J Cell Sci 131. https://doi.org/10.1242/jcs.203208

Herburger K, Xin A, Holzinger A (2019) Homogalacturonan Accumulation in Cell Walls of the Green Alga *Zygnema* sp. (Charophyta) Increases Desiccation Resistance. Front Plant Sci. https://doi.org/10.3389/fpls.2019.00540

Hill AE, Shachar-Hill B, Skepper JN, Powell J, Shachar-Hill Y (2012) An Osmotic Model of the Growing Pollen Tube. PLoS One 7:e36585. https://doi.org/10.1371/journal.pone.0036585

Holzinger A, Karsten U (2013) Desiccation stress and tolerance in green algae: consequences for ultrastructure, physiological, and molecular mechanisms. Front Plant Sci 4. https://doi.org/10.3389/fpls.2013.00327

Holzinger A, Pichrtova M (2016) Abiotic Stress Tolerance of Charophyte Green Algae: New Challenges for Omics Techniques. Front Plant Sci 7. https://doi.org/10.3389/fpls.2016.00678

Hsu SY, Kao CH (2003) Differential effect of sorbitol and polyethylene glycol on antioxidant enzymes in rice leaves. Plant Growth Regul 9: 83–90. https://doi.org/10.1023/A:1021830926902

Ji H, Liu L, Li K, Xie Q, Wang Z, Zhao X, Li X (2014) PEG-mediated osmotic stress induces premature differentiation of the root apical meristem and outgrowth of lateral roots in wheat. J Exp Bot 65: 4863–4872. https://doi.org/10.1093/jxb/eru255

Jiao C, Sørensen I, Sun X, Sun H, Behar H, Alseekh S, Philippe G, Palacio-Lopez K, Reed R, Jeon S, Kiyonami R, Zhang S, Fermie AR, Brumer H, Domozych DS, Fei Z, Rose JKC (2020) The Genome of the Charophyte Alga *Penium margaritaceum* Bears Footprints of Terrestrialization and Preludes the Evolutionary Origins of Land Plants. Cell 181:1097–1111.e12. https://doi.org/10.1016/j.cell.2020.04.019

Kaplan F, Lewis LA, Herburger K, Holzinger A (2012a) Osmotic stress in Arctic and Antartic strains of the green alga *Zygnema* (Zygematales, Streptophyta): Effects on photosynthesis and ultrastructure. Micron 44:317–330. https://doi.org/10.1016/j.micron.2012.08.004

Kaplan F, Lewis LA, Wastian J, Holzinger A (2012b) Plasmolysis effects and osmotic potential of two phylogenetically distinct alpine strains of *Klebsormidium* (Streptophyta). Protoplasma 249:789–804. https://doi.org/10.1007/s00709-011-0324-z

Kim S-J, Brandizzi F (2014) The Plant Secretory Pathway: An Essential Factory for Building the Plant Cell Wall. Plant Cell Physiol 55:687–693. https://doi.org/10.1093/pcp/pct197

Komatsu S, Konishi H, Hashimoto M (2007) The proteomics of plant cell membranes. J Exp Bot 58:103–112. https://doi.org/10.1093/jxb/erj209

Lamport DTA, Tan L, Held MA, Kieliszewski J (2018) Pollen tube growth and guidance: Occam's razor sharpened on a molecular arabinogalactan glycoprotein Rosetta Stone. New Phytol 217:491–500. https://doi.org/10.1111/nph.14845

Landrein B, Ingram G (2019) Connected through the force: mechanical signals in plant development. *J Exp Bot* 70:3507–3519. https://doi.org/10.1093/jxb/erz103

Lang I, Barton DA, Overall RL (2004) Membrane-wall attachements in plasmolyzed plant cells. Protoplasma 224:231–243. https://doi.org/10.1007/s00709-004-0062-6

Lang I, Sassmann S, Schmidt B, Komis G (2014) Plasmolysis: Loss of Turgor and Beyond. Plants 3:583–593

Leroux O, Leroux F, Bagniewska-Zadworna A, Knox JP, Claeys M, Bals S, RLL V (2011) Ultrastructure and composition of cell wall appositions in the roots of *Asplenium* (Polypodiales). Micron 42:863–870. https://doi.org/10.1016/j.micron.2011.06.002

Li X, Bao H, Wang Z, Wang M, Fan B, Zhu C, Chen Z (2018) Biogenesis and Function of Multivesicular Bodies in Plant Immunity. Front Plant Sci 9:979. https://doi.org/10.3389/fpls.2018.00979

Lin Y, Ding Y, Wang J, Shen J, Kung CH, Zhuang X, Cui Y, Yin Z, Xia Y, Lin H, Robinson DG, Jiang L (2015) Exocyst-Positive Organelles and Autophagosomes Are Distinct Organelles in Plants. Plant Phyiol 169:1917–1932. https://doi.org/10.1104/pp.15.00953

Liu Z, Persson S, Sánchez-Rodríguez C (2015) At the border: the plasma membrane–cell wall continuum. J. Expt Bot 66:1553–1563. https://doi.org/10.1093/jxb/erv019

Lopez-Hernandez F, Tryfona T, Rizza A, Yu XL, Harris MOB, Webb AAR, Kotake T, Dupree P (2020) Calcium Binding by Arabinogalactan Polysaccharides Is Important for Normal Plant Development. Plant Cell 32:3346–3369. https://doi.org/10.1105/tpc.20.00027

Luschnig C, Vert G (2014) The dynamics of plant plasma membrane proteins: PINs and beyond. Development. 14:2924–2938. https://doi.org/10.1242/dev.103424

Lütz-Meindl U (2016) *Micrasterias* as a Model System in Plant Cell Biology. Front Plant Sci 7. https://doi.org/10.3389/fpls.2016.00999

Maleki SS, Mohammadi K, Ji KS (2016) Characterization of Cellulose Synthesis in Plant Cells. Sci World J 2016:8641373–8641378. https://doi.org/10.1155/2016/8641373

Masclaux-Daubresse C (2017) Regulation of nutrient cycling via autophagy. Cur Opin Plant Biol 39:8–17. https://doi.org/10.1016/j.pbi.2017.05.001

Novakovic L, Guo T, Bacic A, Sampathkumar A, Johnson KL (2018) Hitting the Wall-Sensing and Signaling Pathways Involved in Plant Cell Wall Remodeling in Response to Abiotic Stress. Plants 7:89. https://doi.org/10.3390/plants7040089

Ochs J, LaRue T, Tinaz B, Yongue C, Domozych DS (2014) The Cortical Cytoskeletal Network and Cell-wall Dynamics in the Unicellular Charophycean Green Alga *Penium margaritaceum*. Ann Bot 114:1237–1249. https://doi.org/10.1093/aob/mcu013

Osakabe Y, Arinaga N, Umezawa T, Katsura S, Nagamachi K, Tanaka H, Ohiraki H, Yamada K, Seo S-U, Abo M, Yoshimura E, Shinozaki K, Yamaguchi-Shinozaki K (2013) Osmotic Stress Responses and Plant Growth Controlled by Potassium Transporters in *Arabidopsi*. Plant Cell 25:609–624. https://doi.org/10.1105/tpc.112.105700

Osmolovskaya N, Shumilina J, Kim A, Didio A, Grishina T, Bilova T, Keltsieva OA, Zhukov V, Tikhonovich I, Tarakhovskaya E, Frolov A, Wessjohann LA (2018) Methodology of Drought Stress Research: Experimental Setup and Physiological Characterization. Int J Mol Sci 19:4089. https://doi.org/10.3390/ijms19124089

Overdijk EJR, Tang H, Borst JW, Govers F, Ketelaar T (2020) Time-gated confocal microscopy reveals accumulation of exocyst subunits at the plant–pathogen interface. J Exp Bot 71:837–849. https://doi.org/10.1093/jxb/erz478

Pecenková T, Markovic V, Sabol P, Kulich I, Žárský V (2018) Exocyst and autophagy-related membrane trafficking in plants. J Exp Bot 69:47–57. https://doi.org/10.1093/jxb/erx363

Palacio-Lopez K, Tinaz B, Holzinger A and Domozych DS (2019) Arabinogalactan Proteins and the Extracellular Matrix of Charophytes: A Sticky Business. Front Plant Sci. https://doi.org/10.3389/fpls.2019.00447

Palacio-Lopez SL, Reed R, Kang E, Sørensen I, Rose JKC, Domozych DS (2020) Experimental Manipulation of Pectin Architecture in the Cell Wall of the Unicellular Charophyte, *Penium Margaritaceum*. Front Plant Sci 11. https://doi.org/10.3389/fpls.2020.01032

Pierre-Jerome E, Drapek C, Benfey PN (2018) Regualtion of Division and Differentiation of Plant Cells. Ann Rev Cell and Devel Biol 34:289–310. https://doi.org/10.1146/annurev-cellbio-100617-062459

Pietruszka M (2013) Pressure-induced cell wall instability and growth oscillations in pollen tubes. PLoS One 8:e75803. https://doi.org/10.1371/journal.pone.0075803

Polko JK, Kieber JJ (2019) The Regulation of Cellulose Biosynthesis in Plants. Plant Cell 2019 3:282–296. https://doi.org/10.1105/tpc.18.00760

Pont-Lezica RF, McNally JG, Pickard BG (1993) Wall-to-membrane linkers in onion epidermis: some hypotheses. Plant Cell Environ 16:111–123. https://doi.org/10.1111/j.1365-3040.1993.tb00853.x

Qi H, Xia F-N, Xiao S (2020) Autophagy in plants: Physiological roles and post-translational regulation. J Integr Plant Biol 63:161–179. https://doi.org/10.1111/jipb.12941

Rao S, FTZ J (2013) In Vitro selection and characterization of polyethylene glycol (PEG) tolerant callus lines and regeneration of plantlets from the selected callus lines in sugar cane (*Saccharum officinarum* L.). Physiol Mol Biol Plants 19:261–268. https://doi.org/10.1007/s12298-013-0162-x

Rensing SA (2018) Great moments in evolution: the conquest of land by plants. Curr Opin Plant Biol 42:49–54. https://doi.org/10.1016/j.pbi.2018.02.006

Rippin M, Becker B, Holzinger A (2017) Enhanced Desiccation Tolerance in Mature Cultures of the Streptophytic Green Alga *Zygnema circumcarinatum* Revealed by Transcriptomics. Plant Cell Physiol 58:2067–2084. https://doi.org/10.1093/pcp/pcx136

Rodriguez-Furlan C, Minina EA, Hicks GR (2019) Remove, Recycle, Degrade: Regulating Plasma Membrane Protein Accumulation. Plant Cell 31:2833–2854. https://doi.org/10.1105/tpc.19.00433

Rui Y, Dinneny JR (2020) A wall with integrity: Surveillance and maintenance of the plant cell wall under stress. *New Phytol* 225:1428–1439. https://doi.org/10.1111/nph.16166

Ruiz-May E, Sørensen I, Fei Z, Zhang S, Domozych DS, Rose JC (2018) The Secretome and N-Glycosylation Profiles of the Charophycean Green Alga, *Penium margaritaceum*, Resemble Those of Embryophytes. Proteomes. 10:3390/proteomes6020014

Rydahl MG, Fangel JU, Mikkelsen MD, Johansen IE, Andreas A, Harholt J, Ulvskov JB, Domozych DS, Willats W (2015) *Penium margaritaceum* as a model organism for cell wall analysis of expanding plant cells. Methods Mol Biol 1242:1–21. https://doi.org/10.1007/978-1-4939-1902-4_1

Shao R, Xin L, Mao J, Li L, Kang G, Yang Q (2015) Physiological, Ultrastructural and Proteomic Responses in the Leaf of Maize Seedlings to Polyethylene Glycol-Stimulated Severe Water Deficiency. Int J Mol Sci 16:21606–21625. https://doi.org/10.3390/ijms160921606

Slama I, Ghnaya T, Hessini K, Messedi D, Savoure A, Abdelly C (2007) Comparative study of the effects of mannitol and PEG osmotic stress on growth and solute accumulation is Sesuvium portulacastrum. Environ Exp Bot 61:10–17. https://doi.org/10.1016/j.envexpbot.2007.02.004

Sørensen I, Domozych D, Willats WG (2010) How have plant cell walls evolved? Plant Physiol 153:366–372. https://doi.org/10.1104/pp.110.154427

Sørensen I, Pettolino FA, Bacic A, Ralph J, Lu F, O'Neill MA, Fei Z, Rose JKC, Domozych DS, Willats WGT (2011) The charophycean green algae provide insights into the early origins of plant cell walls. Plant J 68:201–211. https://doi.org/10.1111/j.1365-313X.2011.04686.x

Steiner P, Obwegeser S, Wanner G, Buchner O, Lütz-Meindl U, Holzinger A (2020) Cell Wall Reinforcements Accompany

Chilling and Freezing Stress in the Streptophyte Green Alga *Klebsormidium crenulatum*. Front Plant Sci 11. https://doi.org/10.3389/fpls.2020.00873

Sugimoto-Shirasu K, Carpita NC, McCann MC (2018) The Cell Wall: A Sensory Panel for Signal Transduction. Annual Plant Reviews book series, Volume 10: The Plant Cytoskeleton in Cell Differentiation and Development 2. Fundamental Cytoskeletal Activities. 1002/9781119312994.apr0096

Tenhaken R (2015) Cell wall remodeling under abiotic stress. Front Plant Sci 5:71. https://doi.org/10.3389/fpls.2014.00771

van Doorn WG, Papini A (2013) Ultrastructure of autophagy in plant cells. Autophagy 9:1922–1936. https://doi.org/10.4161/auto.26275

Vaahtera L, Schulz J, Thorsten H (2019) Cell wall integrity maintenance during plant development and interaction with the environment. Nat Plants 5:924–932. https://doi.org/10.1038/s41477-019-0502-0

van Rensberg HCJ, Van den Ende W, Signorelli S (2019) Autophagy in plants: both a puppet and puppet master of sugars. Front Plant Sci. https://doi.org/10.3389/fpls.2019.00014

Wallace G, Fry SC (1994) Pheonolic components of the plant cell wall. Int Rev Cytol 151:229–267. https://doi.org/10.1016/S0074-7696(08)62634-0

Wang L, Ruan Y-L (2013) Regulation of cell division and expansion by sugar and auxin signaling. Front Plant Sci 4. https://doi.org/10.3389/fpls.2013.00163

Wang T, McFarlane HE, Persson S (2016) The impact of abiotic factors on cellulaose synthesis. J Exp Bot 67:543–552. https://doi.org/10.1093/jxb/erv/488

Wang S, Li L, Li H, Sahu SK, Wang H, Xu Y, Xian W, Song B, Liang H, Cheng S, Chang Y, Song Y, Çebi Z, Wittek S, Reder T, Peterson M, Yang H, Wang J, Melkonian B, van de Peer Y, Xu X, Wong GKS, Melkonian M, Liu H, Liu X (2020a) Genomes of early-diverging streptophyte algae shed light on plant terrestrializatiom. Nature Plants 6:95–106. https://doi.org/10.1038/s41477-019-0560-3

Wang X, Xu M, Gao C, Zeng Y, Cui Y, Shen W, Jiang L (2020b) The roles of endomembrane trafficking in plant abiotic stress responses. J Integ. Plant Biol 62:55–69 1111/jpb.12895

Wasteneys GO, Willingale-Theune J, Menzel D (1997) Freeze shattering: a simple and effective method for permeabilizing higher plant cell walls. J Microsc 188:51–61. https://doi.org/10.1046/j.1365-2818.1977.2390796.x

Yang W, Ruan M, Xiang M, Deng A, Du J, Xiao C (2020) Overexpression of a pectin methylesterase gene PtoPME35 from *Populus tomentosa* influences stomatal function and drought tolerance in Arabidopsis thaliana. Biochem Biophys Res Commun 523:416–422. https://doi.org/10.1016/j.bbrc.2019.12.073

Yoneda A, Ohtani M, Katagiri D, Hosokawa Y, Demura T (2020) Hechtian Strands Transmit Cell Wall Integrity Signals in Plant Cells. Plants 9:604. https://doi.org/10.3390/plants9050604

Zeng HY, Zheng P, Wang LY, Bao HN, Sahu SK, Yao N (2019) Autophagy in plant immunity. Adv Exp Med Biol 1209:23–41. https://doi.org/10.1007/978-981-15-0606-2_3

Zheng X, Wu M, Li X, Cao J, Li J, Wang J, Huang S, Liu Y, Wang Y (2019) Actin filaments are dispensable for bulk autophagy in plants. Autophagy 15:2126–2141. https://doi.org/10.1080/15548627.2019.1596496

Zhang D, Zhang B (2020) Pectin Drives Cell Wall Morphogenesis without Turgor Pressure. Trends Plant Sci 25:719–722. https://doi.org/10.1016/j.tplants.2020.05.007

Zhang L, Xing J, Lin J (2019) At the intersection of exocytosis and endocytosis in plants. New Phytol 224:1479–1489. https://doi.org/10.1111/nph.16018

Zhu J-K (2016) Abiotic Stress Signaling and Responses in Plants. Cell 167:313–324. https://doi.org/10.1016/j.cell.2016.08.029

Zonia L, Munnik T (2007) Life under pressure: hydrostatic pressure in cell growth and function. Trends Plant Sci 12:90–97. https://doi.org/10.1016/j.tplants.2007.01.006

Zonia L, Munnik T (2011) Understanding pollen tube growth: the hydrodynamic model versus the cell wall model. Trends Plant Sci 7:1–6. https://doi.org/10.1016/j.tplants.2011.03.009

Zwieka M, Nodzynski T, Robert S, Vanneste S (2015) Osmotic Strerss Modulates the Balance between Exocytosis and Calthrin-Mediated Endocytosis inn *Arabidopsis thaliana*. Mol Plant 8:1175–1187. https://doi.org/10.1016/j.molp.2015.03.007